5-2021

Sensitivity and threshold dynamics of Pinus strobus and Quercus spp. in response to experimental and naturally-occurring severe droughts

Heidi Asbjornsen
University of New Hampshire

Cameron D. McIntire
USDA Forest Service

Matthew A. Vadeboncoeur
University of New Hampshire, Durham, matt.vad@unh.edu

Katie A. Jennings
University of New Hampshire, Durham

Adam P. Coble
University of New Hampshire, Durham

See next page for additional authors

Recommended Citation

Asbjornsen H, McIntire CD, Vadeboncoeur MA, Jennings KA, Coble AP, Berry ZC. Sensitivity and threshold dynamics of Pinus strobus and Quercus spp. in response to experimental and naturally-occurring severe droughts. Tree Physiology, 41(10): 1819-1835. doi:10.1093/treephys/tpab05

Sensitivity and threshold dynamics of *Pinus strobus* and *Quercus spp.* in response to experimental and naturally-occurring severe droughts

Heidi Asbjornsen [1,2 *]
Cameron D. McIntire [1,3 *]
Matthew A. Vadeboncoeur [2 *]
Katie A. Jennings [1,2]
Adam P. Coble [1,4]
Z. Carter Berry [1,5]

1. Department of Natural Resources and the Environment, University of New Hampshire, Durham, NH 03824 USA
2. Earth Systems Research Center, University of New Hampshire, Durham, NH 03824 USA
3. USDA Forest Service, State and Private Forestry, Durham, NH 03824 USA
4. Private Forests Division, Oregon Department of Forestry, Salem, OR 97310 USA
5. Schmid College of Science and Technology, Chapman University, Orange, CA 92866 USA

* these authors contributed equally to this manuscript

Author contributions: HA, CDM, and MAV designed the study. CDM, KAJ, MAV, APC, and ZCB conducted field and lab work and analyzed data. HA led the writing with major contributions from CDM and MAV. All authors contributed to interpreting results and writing the manuscript. The authors declare no conflicts of interest.

ABSTRACT

Increased drought frequency and severity are a pervasive global threat, yet the capacity of mesic temperate forests to maintain resilience in response to drought remains poorly understood. We deployed a throughfall removal experiment to simulate a once in a century drought in New Hampshire, USA, which coupled with the region-wide 2016 drought, intensified moisture stress beyond that experienced in the lifetimes of our study trees. To assess the sensitivity and threshold dynamics of two dominant northeastern tree genera (*Quercus* and *Pinus*), we monitored sap flux density (J_s), leaf water potential and gas exchange, growth, and intrinsic water use efficiency (iWUE) for one pretreatment year (2015) and two treatment years (2016-17). Results showed that J_s in pine (*P. strobus*) declined abruptly at a soil moisture threshold of 0.15 m^3m^{-3}, while oak's (*Q. rubra* and *Q. velutina*) threshold was 0.11 m^3m^{-3} — a finding consistent with pine's more isohydric strategy. Nevertheless, once oaks' moisture threshold was surpassed, J_s declined abruptly, suggesting that while oaks are well-adapted to moderate drought, they are highly susceptible to extreme drought. The radial growth reduction in response to the 2016 drought was more than twice as great for pine than for oaks (50% vs. 18% respectively). Despite relatively high precipitation in 2017, the oaks' growth continued to decline (low recovery), whereas pine showed neutral (treatment) or improved (control) growth. iWUE increased in 2016 for both treatment and control pines, but only in treatment oaks. Notably, pines exhibited a significant linear relationship between iWUE and precipitation across years, whereas the oaks only showed a response during the driest conditions, further underscoring the different sensitivity thresholds for these species. Our results provide new insights into how interactions between temperate forest tree species' contrasting physiologies and soil moisture thresholds influence their responses and resilience to extreme drought.

Introduction

Humid temperate regions globally are expected to become simultaneously wetter (greater mean precipitation) and drier (more prolonged droughts; Huntington et al. 2009, Dai 2013). In the northeastern U.S. (hereafter NE), climate patterns over the past century already reflect these trends, as both the mean and variance of annual precipitation have increased (Krakauer and Lakhankar 2019). During the late summer in 2016, a severe drought affected much of the NE (Sweet et al. 2017, US Drought Monitor 2020), with southeastern New Hampshire experiencing its 11th driest summer since 1895, and the driest since 1993 (Daly et al. 2008). While drought has been implicated in massive tree mortality across all major ecosystems globally (Allen et al. 2010), such reports are rare for the NE, likely reflecting both the historical rarity of extreme drought (Pederson et al. 2014) and the fact that long-lived trees generally have conservative carbon (C) allocation strategies and therefore high stress tolerance (Martin et al. 2017). However, drought tolerance may also depend in part on adaptation to prior drought events (DeSoto et al. 2020). Consequently, we lack a sound understanding of the sensitivity and threshold dynamics of NE temperate forests under extreme drought (Coble et al. 2017). Given the important role of NE forests in carbon storage and other ecosystem services to society (Xiao et al. 2011), and the understudied potential drought vulnerability of species adapted to relatively wet conditions (Isaac-Renton et al. 2018), addressing this knowledge gap is critical to predicting future change and managing forests for climate adaptation.

Two key metrics, stomatal regulation and woody stem growth, have been widely used to assess drought sensitivity across diverse tree species and forest ecosystems. The first, stomatal regulation, is a measure of the degree to which plants adjust stomatal apertures under moisture stress (Oren et al. 1999). Species differences in stomatal sensitivity can be characterized according to their relative position along a continuum of isohydricity (e.g., Klein, 2014), with strongly isohydric species exhibiting tight stomatal control at the cost of reduced C uptake in dry conditions, while anisohydric species tolerate more negative water potentials, which risks damaging their hydraulic architecture. While NE tree species tend to have greater stomatal sensitivity to moisture stress compared to species from drier climates, they fall along a

spectrum from strongly isohydric (e.g., *Acer saccharum*, *Betula alleghaniensis*, *Pinus strobus*, and *Populus tremuloides*) to anisohydric (e.g. *Quercus rubra;* Federer 1980, Kubiske and Abrams 1994, Bovard et al. 2005, Yi et al. 2017). Generally, anisohydric species are considered more drought tolerant than isohydric species (Niinemets and Valladares 2006, Gustafson and Sturtevant 2013, Peters et al. 2015).

Previous studies aimed at assessing the response of NE species to severe drought have been conducted at drier sites located at the southern or western extent of these species' natural ranges (e.g., Dietze and Moorcroft, 2011; Gu et al., 2015; Hoffmann et al., 2011; Meinzer et al., 2013; Yi et al., 2017). An emerging hypothesis suggests greater vulnerability of anisohydric species to severe drought due to catastrophic hydraulic failure; however, this hypothesis remains largely untested, especially for more humid NE forests (Coble et al. 2017). Moreover, empirical observations of drought response can often deviate substantially from predictions derived from the isohydry-anisohydry framework (Adams et al. 2017, Hochberg et al. 2018), underscoring the need for experimentally-based investigations across a broader range of climates and species.

The second metric of drought sensitivity, woody stem growth, provides an integrated measure of how physiological responses affect productivity. Studies using tree rings to retrospectively study growth responses to past climate variability in the NE have yielded mixed results. Some studies identify precipitation as a significant driver of historical variation in tree growth (Abrams et al. 2000, Pederson et al. 2014, Martin-Benito and Pederson 2015, D'Orangeville et al. 2018), while others suggest weak responses to precipitation (Klos et al. 2009, Brzostek et al. 2014, LeBlanc and Berland 2019). Tree ring datasets have distinct advantages for assessing growth response to climate (e.g. long time scales covering a wide range of conditions) but are constrained by potential biases, including (in most cases) sampling only surviving trees (Bowman et al. 2013, Duchesne et al. 2019), and a tendency to sample droughty sites (Cook and Pederson 2011). Despite these limitations, woody growth increment is a useful integrator of tree response to stress, especially when coupled with controlled experimental manipulations (see below).

A useful framework for applying these two metrics of drought sensitivity is through the lens of environmental and physiological thresholds that provoke abrupt changes in ecological response (Groffman et al. 2006, Mitchell et al. 2014, Munson et al. 2020). For example, a growing number of studies have linked nonlinear behavior in tree physiological and growth responses to future die-back (Camarero et al. 2015, Guerin et al. 2018, Mitchell et al. 2014) and mortality (Cavin et al. 2013, Choat et al. 2018, Mamet et al. 2015, De Grandpre et al. 2018, Cailleret et al. 2019, Sánchez -Salguero et al. 2020; but see Billings et al. 2015). Given that significant timelags are often assocated with mortality events in long-lived trees, pronounced nonlinear responses can serve as important early warning signs of imminent future change. This framework can also provide insight about species' resilience to extreme events, both in terms of resistance (capacity to remain unchanged during a disturbance) and recovery (capacity to return to pre-disturbance function) (e.g., Mitchell et al., 2016). Controlled throughfall manipulation experiments are especially well-suited to elucidate threshold responses to extreme drought (Pangle et al. 2012, McDowell et al. 2013, Mitchell et al. 2014, Meir et al. 2015); but are rarely implemented in tall-statured forests (Asbjornsen et al. 2018).

To better understand how NE forests respond to drought, we experimentally imposed a once-in-a-century drought for two years in a southern New Hampshire forest. We measured stomatal regulation and growth response of two co-occurring genera: oak (*Quercus rubra* L. and *Q. velutina* Lam.) and pine (*Pinus strobus* L.). These species have sharply contrasting physiological strategies for managing moisture stress, with *Q. rubra* considered one of the most anisohydric species in NE forests (Choat et al. 2012), while pines generally exhibit isohydric behavior (Niinemets and Valladares 2006, Peters et al. 2015). Previous work suggests that anisohydric species may be more tolerant of moderate drought by maintaining gas exchange functions, but more vulnerable to extreme drought than isohydric species, due to their inability to avoid catastrophic negative water potentials that lead to excessive hydraulic damage (Hoffman et al. 2011, Gu et al. 2015, Kannenberg et al. 2019). Moreover, the fundamentally different wood anatomies and associated water and carbon management strategies of oaks (ring-porous xylem) and pines (tracheids; Olson et al. 2020), combined with their contrasting growth phenologies (e.g., oaks

complete most of their growth earlier in the season whereas pines typically continue their growth later in the season; Vose and Swank 1994, Rossi et al. 2006, LeBlanc and Terrell 2009, McIntire et al. 2020), these species may differ in their sensitivities and lag responses to extreme drought.

Our specific objectives were to (1) assess each species' physiological sensitivity and threshold dynamics in response to severe drought and (2) examine the consequences of drought sensitivity on the woody growth response and recovery in these species. Here, we report results from the first three years of the experiment, including one year of pre-treatment data and the first two years of throughfall removal. The first treatment year, 2016, coincided with a severe drought that affected much of the NE. We hypothesized that (1) oaks would initially exhibit weaker stomatal and growth sensitivity to increasing (moderate) moisture stress than pine; (2) extreme drought conditions would elicit a more pronounced threshold behavior in oaks compared to a more gradual and consistent response in pine; and (3) legacy effects following extreme drought would be greater and recovery slower in oak than pine due to their diverging phenologies and threshold dynamics.

Methods

Study site and species

We conducted this study in a mixed-species mature second-growth forest located at Thompson Farm in Durham, NH (43.11ºN, 70.95ºW, 25 masl). Mean annual temperature and precipitation average 8.6 ºC (1981–2010) and 1165 mm, respectively. Precipitation is evenly distributed throughout the year (Daly et al. 2008). The forest is dominated by an early-successional cohort of eastern white pine (*P. strobus*; hereafter "pine") with a mean establishment date in the 1930s and a younger cohort of oaks (northern red oak, *Q. rubra*; and black oak, *Q. velutina*) that established in the 1960s following forest thinning. These *Quercus* species are closely related within the *Lobatae* oaks (Hipp et al. 2018), often co-occur, and have similar geographic ranges (Burns and Honkala 1990). For simplicity, we refer to both species as "oak" and combine the data, since no significant differences were observed between these species for any response variables. Soils are well-drained Entisols and Inceptisols with a loamy sand to sandy loam

texture. Depth to parent material (unweathered outwash or basal till) is 70 – 100 cm. Roots are found to at least 120 cm depth, but a majority of root biomass is in the upper 30 cm.

Experimental Design

In 2015, we established four 30 x 30 m plots that consisted of two control-treatment pairs located approximately 1 km apart. We selected plots that contained at least three healthy, codominant to dominant pines and three healthy, codominant oaks within 10 meters of the plot center. We avoided sampling trees within 5 m of plot edges to reduce the influence of roots extending beyond the treatment boundaries. Both oak species are present in each plot. Within each pair, one plot was selected for the construction of a passive throughfall exclusion (TFE) structure with 55% coverage by area (Asbjornsen et al. 2018). Beginning in 2016, sloped troughs of 6-mil reinforced clear polyethylene sheeting were installed about two meters aboveground, running from a peaked midline to opposing edges of each plot (Fig. S1). Troughs were installed in late May of each treatment year and removed each November to avoid overloading the structure with snow. Gutters and drainage hoses at each corner diverted captured throughfall at least 5 meters from the plot edge. The targeted 55% reduction in growing-season throughfall was intended to simulate a 1-in-100 year drought (assuming precipitation equal to the long-term mean), consistent with the methodology of the International Drought Experiment (Knapp et al. 2017). We estimate that the troughs reduced total precipitation inputs to the soil by 50% when present (Supplement 1a). The passive design for diverting throughfall from the plot in multiple directions required that the TFE plots be located in slightly convex landscape positions, while comparably sized and spaced control trees were located in flat or mid-slope positions nearby.

Soil moisture and climate data

Beginning in May 2015, soil volumetric water content (VWC, m^3m^{-3}) was measured every 15 minutes at four locations per plot, at depths of 10, 20, and 30 cm using 5TM sensors (Meter, Pullman, WA, USA). Sensor locations in TFE plots were stratified to equally represent areas under troughs and under gaps.

Meteorological data (15-minute temperature, precipitation, relative humidity, wind, solar radiation) have been collected since 2010 at a U.S. Climate Reference Network station (WBAN #54795; NH Durham 2 SSW) located in a mowed field within 700 m of all study plots. Similar data were collected above the forest canopy at a height of 32 m, on a flux tower within 500 m of all study plots (Sanders-DeMott et al. 2020).

Sap flow

Beginning in 2015, we used heat-ratio sensors (Burgess et al. 2001) to measure sap flux density (J_s) every 15 minutes, in three pines and three oaks per plot. Sensors were constructed in our lab, with a maximum thermocouple depth of 35mm in the pines and 15-35mm in the oaks (Supplement 1b). One set of sensors was installed per tree at approximately breast height, and subsequent installation sites were moved at least 10 cm around the circumference of the tree. Sap flow was generally monitored from early June through late September each year, though sensors were removed in early September 2015 to allow for throughfall exclusion structure construction. Details on data collection and processing are provided in Supplement 1b. As our main goal was to contrast species' time course of response to drought events, we focus on relativized metrics of sap flux density, rather than upscaled total water use.

Leaf water potential

Mid-day leaf water potentials were measured on 18–19 July and 22–24 August 2016 between 10:00 and 14:00 EDT. Individual leaves of oaks and the distal twigs of pine were measured using a Scholander-type pressure chamber (PMS instruments Model 1505D). Sun-exposed twig segments containing intact fascicles and leaves were collected from the upper canopy using a 12-gauge shotgun. We sampled n=3 trees per species in each plot. The average of n=2 water potential measurements conducted within ~5 min for each tree is used for analysis.

Leaf gas exchange

Leaf gas exchange was measured on 13–14 Aug 2015, 22–24 Aug 2016, and 21–22 Aug 2017 using a portable photosynthesis system (LI-6400XT, Li Cor, Inc., Lincoln, NE). Samples were collected with a shotgun under clear skies between 10:00 – 14:00 EDT. Measurements were conducted immediately, with photosynthetically active radiation (PAR) of 2000 μmol m^{-2} s^{-1}, and [CO_2] of 400 ppm, while ambient chamber temperature and relative humidity ranged 24 – 29 °C and 30 – 50%, respectively. Samples were collected using a shotgun, and twigs were immediately cut under water (Venturas et al. 2015). For pine, two complete second-year fascicles (consisting of ten intact needles) were placed parallel to the long side of the 6.0 cm^2 cuvette for gas exchange measurements. Once photosynthesis (A) and stomatal conductance (g_s) stabilized (2–15 min), five instantaneous measurements were taken over a 30 second period and averaged. Gas exchange rates of pine foliage were corrected using projected area measured using a flatbed scanner at 1200 dpi and ImageJ (Katabuchi 2015). Intrinsic water use efficiency (iWUE) is calculated as A/g_s.

Tree growth

We collected increment cores twice during the study period, first in 2015 to characterize stand age structure and disturbance history, and shorter cores (~5 cm depth) in October 2017 to assess post-treatment responses. Each time, one core was taken from each codominant pine and oak in the central 20 x 20 meters of each plot (46 trees total; 9–15 per species per treatment). Samples were collected with 5.15 mm-diameter borers, at 30–50 cm height (just above any root flare) to avoid affecting sap flow at breast height.

The 2015 cores were cross-dated using standard methods (Speer 2010). While the second set of cores was too short to cross-date, our 2015 analysis provided recent marker years for validation. To assess treatment effects on growth, we calculated the mean basal area increment (BAI; cm^2) of each tree prior to the start of the experiment (2011–15) as a pre-treatment baseline.

Water use efficiency from tree-core isotopes

Stable C isotopes of tree rings allow retrospective estimates of iWUE (McCarroll and Loader 2004). We extracted latewood α-cellulose (Leavitt and Danzer 1993) for 2016, 2017, and a composite sample of the latewood from the 2011-15 pre-treatment period, from 6 trees per genus per treatment. Samples were analyzed on an Isoprime IRMS for stable C isotope ratios. We calculated discrimination (Δ; Farquhar et al. 1982) relative to the atmosphere (Mauna Loa Sampling Station Record 2018). Discrimination is linearly related to the ratio of leaf intracellular [CO_2] to atmospheric [CO_2] (c_i/c_a; Farquhar et al., 1989) and is a useful proxy for iWUE when the effect of increasing atmospheric CO_2 is not of direct interest (Mathias and Thomas 2018). Longer-term composite $\delta^{13}C$ chronologies from these plots were reported by Vadeboncoeur et al. (2020).

Statistical Analysis

Due to the low level of true replication (2 plots per treatment), we treat individual trees as pseudoreplicates for the purposes of detecting treatment effects. The three oak replicates in one of our control plots exhibited very low sap flux densities across all three years including the pre-treatment year (Supplement 1b). We excluded these trees from physiological analysis and use a replication of $n = 3$ for control oaks, while all other species/treatment replication is $n = 6$.

The correlation of mean daily sap flux density (J_s) to soil volumetric water content (VWC) was assessed only for days in which VPD was greater than 0.4 kPa, mean daytime photosynthetic photon flux density was greater 300 μmol m^{-2} s^{-1}, and with 0 mm precipitation. These criteria exclude days when transpiration was strongly limited by non-physiological factors, which decouples water use from the influence of soil water status. This analysis includes a total of 74, 97, and 79 days used for 2015, 2016 and 2017 respectively, while all days ($n = 250$) and years are pooled for regression fits. Sap flux data in 2017 are sparse due to instrument failure. For this analysis we assessed an integrated average soil moisture profile between the 10 to 30 cm depth. A piecewise linear regression analysis was fit for each species using the 'segmented' package in R (Muggeo 2008). This analysis estimated slopes and breakpoints for the two segmented regression models, thus identifying significant thresholds for which J_s

begins to decline with decreasing soil moisture during drought for each species. ANCOVA was used to compare slopes of the segmented regression between treatments and species and an independent *t*-test using the overlap of the 83% confidence intervals derived from the breakpoint standard errors was used to compare the breakpoint value between species.

We also assessed the relationship of a normalized mean daily J_s to the calculated reference evapotranspiration (ET_0). The daily ET_0 was calculated using the Penman-Monteith equation (FAO-56 method, Zotarelli et al., 2010) and high-frequency, above-canopy meteorology from the nearby flux tower. Mean daily J_s was normalized using the mean value for daily J_s in the month of June of each year for each species within their respective plots (Table S1). This normalized metric for J_s standardizes sap flux to the relatively mesic conditions in the early growing season of each year. For this analysis we include all available days of sap flux data in each treatment year (130 and 111 days in 2016 and 2017 respectively). The slopes of simple linear regressions for each genus were compared between the control and treatment to determine effects of throughfall removal on J_s. The regression was fit on a plot basis (n = 3 trees per genus per plot). Separate regressions were fit based on the determination of a soil water content breakpoint (described above); the value of VWC for which we believe trees of each species become sensitive to soil water status. The purpose of this analysis was to test whether droughted trees are decoupled from atmospheric drivers of transpiration and assess differences in species sensitivity to drought. Thus, we expected that trees within the treatment plots would have a weaker correlation with ET_0 during the driest parts of the year. Analysis of covariance (ANCOVA) was conducted in R v3.5.1 (R Core Team 2017) using ET_0 as a covariate to the normalized J_s data while the treatment (control, TFE) is defined as an independent variable.

Treatment effects on growth in each post-treatment year were assessed using *t*-tests on the ratio basal area increment to the pre-treatment baseline. Effects of the 2016 drought event for each genus in each treatment are expressed as the mean basal area increment ratio and tested for significance (difference from a ratio of 1.0) with a one-sample *t*-test. Treatment and natural drought effects on Δ were tested in the same way.

Results

Meteorological conditions

Relative to long-term means, our pre-treatment year (2015) was dry, and the US Drought Monitor classified the area as experiencing moderate drought in May, June, and September. Precipitation was again below normal in 2016 (Fig. S2), with moderate drought developing in early June, severe drought by mid-July, and extreme drought in September (US Drought Monitor 2020). In contrast, precipitation was above average in spring 2017, then average throughout the growing season (Fig. S2). Our throughfall exclusion treatments exacerbated precipitation deficits in 2016 (assuming they removed 50% of inputs, these plots were drier than any comparable period in the past 124 years), while in 2017 even the treatment plots received more total precipitation by September than did the control plots in either of the two preceding years (Fig. S2). This interannual variability allowed us to compare the effects of a wide range of precipitation amounts.

June-September daily maximum vapor-pressure deficit (VPD_{max}) averaged 1.85 kPa in 2015 (65th percentile), 2.07 kPa in 2016 (94th percentile), and 1.73 kPa in 2017 (33rd percentile), based on PRISM interpolations for 1895-2018. Six-month Standardized Precipitation-Evapotranspiration Index (SPEI) in August and September 2016 averaged -2.0, making this time period drier than 98% of all months since 1950 (Beguería et al. 2020). SPEI indicates less extreme dry conditions (around -1.0; 20th percentile) in late summer 2015. In contrast, SPEI was positive (i.e. wetter than average) in 2017.

Stomatal regulation of transpiration

During the first treatment year (2016), both species exhibited declining sap flow during periods of low rainfall and soil drying (Fig. 1). Treatment trees for both species had greater declines in sap flow than control trees and maintained near-zero sap flow at the peak of the drought in early September 2016. However, oaks maintained a greater relative difference between control and treatment trees compared to the pines, which lasted until late August when the drought became more severe. At this time, J_s of oak

treatment trees declined abruptly, consistent with a stronger threshold behavior. Late in the 2017 growing season, J_s values were overall greater and differences between drought and control trees were muted relative to 2016.

Notably, there were some pre-treatment differences in soil moisture and J_s that we had to account for. Pre-treatment soil moisture was inherently lower in treatment plots relative to control plots (Fig. 1 G, H & I) leading to lower pre-treatment J_s values. Additionally, absolute J_s for oak during 2015 was much lower than the proceeding two years. This could have been due to our changes to sensor design to more optimally measure fluxes in the shallow sapwood of *Quercus* species, though the application of a correction for sap flow measurement depth did not substantially affect this pattern (Supplement 1b, Fig. S3). Consequently, in order to account for these pre-treatment differences in soil moisture and J_s and facilitate comparisons among years and species, we normalized the J_s data based on the mean J_s during June (i.e., period of maximum J_s) for all relevant analyses described below (i.e., regression analysis between J_s and ET_0).

Diurnal patterns of J_s (Fig. S4) earlier and later in the 2016 growing season demonstrate that pine J_s declined rapidly as VPD increased by midday, compared to a more gradual (hump-shaped) reduction in oak J_s. These patterns reflect pine's greater stomatal sensitivity to increasing atmospheric demand later in the day. This suggests that oaks exhibited more abrupt threshold responses to atmospheric drivers. As expected, diurnal J_s curves of treatment trees later in the growing season were suppressed relative to control trees. As the drought intensified, J_s values are correspondingly lower for both treatments and species relative to the early season.

A breakpoint analysis was conducted to further explore the role of soil moisture thresholds in controlling the physiological responses among the study species (Fig. 2). The breakpoint soil moisture was significantly higher for pine (0.15 m^3m^{-3} VWC) than for oaks (0.11 m^3m^{-3} VWC), suggesting that pine began to exhibit a strong sensitivity to soil moisture sooner than oak. An ANCOVA showed that the slopes differed by species both above ($F(1, 952) = 9.71$, $p = 0.002$) and below ($F(1, 617) = 6.46$, $p = 0.011$) the breakpoint, indicating that pine sap flow declined more rapidly after the soil moisture threshold

was reached and as drought intensified later in the season. Both species reached near-zero J_s values at similar thresholds (0.08–0.09 m^3m^{-3} VWC). The R^2 values for the pine and oaks above the VWC breakpoint were fairly low (R^2 = 0.11 and 0.08, respectively), consistent with atmospheric demand exerting greater controls on transpiration than soil moisture. In contrast, regressions below the breakpoint were highly significant (p<0.001) for both pine (R^2 = 0.41) and oak (R^2 = 0.22).

We find that when VWC is high and soil moisture non-limiting (above the breakpoint), the relationship between normalized J_s and ET_0 (Fig. 3) is the same for both pine (F(1,187) = 2.48, p = 0.117) and oak (F(1,316) = 1.06, p = 0.303). In contrast, when VWC is below the breakpoint, both the slopes (m) and the correlation with ET_0 are lower for both pine (control: m = 0.16, R^2 = 0.67; treatment: m = 0.11, R^2 = 0.40) and oak (control: m = 0.13, R^2 = 0.74; treatment: m = 0.09, R^2 = 0.45). ANCOVA showed that regression fits differed by treatment for both pine (F(1,260) = 6.22, p = 0.013) and oak (F(1,133) = 4.42, p = 0.037), again suggesting that J_s becomes decoupled from atmospheric drivers and more strongly controlled by soil moisture during drought.

For each species and by treatment, we investigated the number of days during the 2016 growing season for which J_s approached zero flow (excluding days in which atmospheric drivers of VPD, PAR, and precipitation limited potential evapotranspiration). We defined this "near zero flow state" as mean daily (24 h) J_s < 5.0 g m^{-2} s^{-1} for pine, and < 2.0 g m^{-2} s^{-1} for oak, as their maximum values of J_s differ by a factor of ~2.5. We found that under these criteria pine exhibited a total of 15 days of near-zero transpiration in the TFE treatment, while trees within the control plots did not drop below 5.0 g m^{-2} s^{-1}. Oak exhibited 26 days of near-zero transpiration within the TFE treatments and no days below this threshold in the control plots. For treatment pines, these days occurred between 30 August and 18 September, coinciding with the driest period. Similarly, treatment oaks exhibited near-zero flow rates throughout this same time period, accounting for 58% of all near-zero days. Interestingly, pine treatment trees were able to recover from this late-season drought following a substantial (9.9 mm) precipitation event on 19 September by again upregulating its transpiration, while oak treatment trees continued to

maintain very low J_s (< 2.0 g m^{-2} s^{-1}) for the remainder of the measurement period into the first week of October 2016 (Fig. 1 B & E).

Leaf water potential

A three-way factorial ANOVA was conducted to test for differences in leaf water potential between treatment (control, TFE), species (pine, oak), and month (July, August). We detected no treatment effect nor any interactions with treatment ($p > 0.05$) (Fig. S5). Only the univariate effects of month ($p = 0.01$) and species ($p = 0.01$) were significant (Table S2). Post-hoc analysis showed significant species differences in Ψ_{leaf} in August 2016 ($p = 0.002$) via a two-tailed *t*-test (Fig. S5), where mean pine Ψ_{leaf} = -1.9 MPa (range -1.5 to -2.2) and mean oak Ψ_{leaf} = -2.2 MPa (range -1.6 to -2.9). These species differences are consistent with oaks' presumed anisohydric behavior, as they exhibited a wider range (and more negative) of leaf water potential. Measurements of leaf water potential were not taken during the peak of the drought in early September 2016, so we are unable to assess whether drier conditions may have exacerbated the differences between treatments or species.

Stomatal regulation from leaf gas exchange

We found that *A* declined significantly in treatment pines in both 2016 ($t(9.1) = 1.85$, $p = 0.048$) and 2017 ($t(6.0) = 1.99$, $p = 0.047$), while oak *A* significantly declined in 2016 only ($t(4.9) = 2.08$, $p = 0.046$), relative to control trees (Fig. 4). This suggests tighter stomatal regulation in pine relative to oaks. Overall, mean stomatal conductance in pine during August of the pre-treatment year was 0.08 mol m^{-2} s^{-1}, while oak g_s was considerably higher at 0.23 mol m^{-2} s^{-1}. Mirroring the results of *A*, pine g_s within treatment plots was significantly lower than control pines for both 2016 ($t(7.8) = 2.70$, $p = 0.014$) and 2017 ($t(8.0) = 2.09$, $p = 0.035$). For oaks, we found no significant difference in g_s between treatments in 2016 or 2017. However, oak g_s in 2016 was markedly lower at 0.06 mol m^{-2} s^{-1}, compared to 0.23 and 0.22 mol m^{-2} s^{-1} in 2015 and 2017, respectively. The iWUE for pine measured in August 2016 was significantly higher in the treatment ($t(5.4)$, $t = -2.53$, $p = 0.024$). In contrast, WUE for oak control and treatment trees did not differ

significantly. The two-tailed *t*-test revealed no difference in pre-treatment *A*, g_s, or WUE between TFE and control plots for either species (Table S3).

Hydraulic vulnerability curves

Hydraulic vulnerability curves constructed for canopy trees in control plots (Supplement 1c) revealed physiologically meaningful species differences (Fig. S6). The P_{50} value for oak was -3.31 MPa (95% confidence interval -2.11 – -4.57 MPa) while that for pine was -5.25 MPa (95% confidence interval -4.75 – -5.99 MPa). Previously published P_{50} values for *Q. rubra* and *Q. velutina* oak range from -1.61 (Maherali et al. 2006) to -2.5 MPa (Cochard and Tyree 1990, Kannenberg et al. 2019). Fewer data are available for *P. strobus,* but Wubbels (2010) reported P_{50} values of -3.0 – -3.6 MPa.

Growth sensitivity

Tree rings show that both pines and oaks grew less in 2016 relative to the pre-treatment period (2011–15), with pine growth reduced by 50% in the control plots and 53% in the treatment plots, while oak growth was reduced by 18% in the control plots and 29% in the treatment plots (Fig. 5). Relative to 2016, pine growth in 2017 was similar (treatment) or slightly increased (control), while oaks in both the control and treatment plots grew even less than in 2016 (33% and 37% below pre-treatment, respectively). Differences between control and treatment trees within each year were not significant for any of the species. These results suggest a trend towards recovery from the 2016 drought in control pines, and possibly a post-drought lag effect leading to continued growth declines in the oaks.

Stomatal regulation inferred from C isotopes

Stable C isotope analyses of tree rings indicate that overall, pines discriminated less against assimilating ^{13}C (Δ), reflecting their higher intrinsic water use efficiency (Fig. 5), consistent with pine's isohydric stomatal regulation strategy and larger hydraulic safety margin. Both control and treatment pine latewood Δ decreased significantly (i.e., increased in iWUE) in 2016, while only treatment plot oaks

showed a significant decrease in Δ relative to the pretreatment values. In 2017, control pines returned roughly to the pre-treatment Δ, while treatment trees increased slightly but remained significantly lower than control trees and pre-treatment values. In contrast, both control and treatment oak Δ were similar to pretreatment values in 2017. After normalizing each tree to its pre-treatment value, treatment tree Δ only differed significantly from control trees among the oaks in 2016 ($p = 0.02$). To further explore relationships between iWUE and precipitation, we plotted Δ against June – September precipitation (Fig. 6). This analysis shows a significant linear relationship ($p = 0.03$; $R^2 = 0.73$) for pine but no significant relationship for oak ($p = 0.44$; $R^2 = 0.15$), suggesting different thresholds in sensitivity for these species, with oak iWUE apparently sensitive only below a threshold of ~150 mm, while pine iWUE is clearly sensitive below ~300 mm.

Discussion

In a simulated once-in-a-century drought, we found threshold changes in stomatal regulation and growth responses that varied by species. Pine exhibited greater sensitivity than the oaks to changing moisture availability, as reflected in pine's J_s closely tracking rainfall events and fluctuations in soil VWC, stricter stomatal regulation, and more pronounced growth reduction during the severe drought of 2016. While oak was less responsive to initial soil drying, oak's water use declined rapidly below its moisture threshold, suggesting relatively strong sensitivity to severe drought.

These findings support our hypothesis that species with strong anisohydric behavior, such as ring-porous oaks (Roman et al. 2015), although well-suited for moderate drought, may leave oaks vulnerable to severe drought. The contrasting growth recovery patterns observed in pine (rapid recovery) versus the oaks (slower recovery) the year following the severe drought are consistent with our second hypothesis, that greater drought-induced declines in physiological function in anisohydric species may delay recovery. Notably, although we observed clear threshold responses in both physiological and growth parameters, and numerous studies have linked such threshold responses to mortality (McDowell et al. 2008, 2013, Plaut et al. 2012, Anderegg et al. 2016), we did not observe any mortality of mature trees in

our plots. Continued monitoring will be essential to understanding the implications for long-term resilience to severe drought in these species.

Physiological sensitivity and threshold dynamics under severe drought

We found a clear threshold response to increasing soil moisture deficit during the 2016 natural drought and experimentally intensified drought in both study species. The breakpoint associated with a nonlinear, abrupt decline in J_s occurred at a significantly higher VWC for pine (0.15 m^3m^{-3}) than for the oaks (0.11 m^3m^{-3}). Our soil moisture threshold results fall within the range reported by the relatively few throughfall manipulation studies of such responses in forest ecosystems (0.07 m^3m^{-3} to 0.15 m^3m^{-3}; (Irvine et al. 1998, MacKay et al. 2012, Sánchez-Costa et al. 2015).

Applying the breakpoint analysis allowed us to compare the linkages between water use and environmental drivers above and below the point at which soil moisture becomes limiting to transpiration. Above the breakpoint, the strength of the correlation between J_s and VWC was somewhat greater for pine than oak, indicating that pine's water use is more tightly linked to soil moisture variability (Fig. 2). This pattern is consistent with a recent nearby study of sap flow in pines and oaks (Coble et al. 2020). The greater sensitivity of pine to moisture stress was also reflected in its relatively high midday leaf water potential (Fig. 4) and iWUE (Fig. 5) as moisture stress increased in 2016, while red oak reached more negative water potential and increased iWUE to a lesser extent under moderate drought. Combined, these patterns are consistent with pine's isohydric strategy, whereby stomata tightly regulate water loss in response to increasing moisture stress at the expense of reduced C assimilation. Conifers, which have a tracheid vascular system that is highly resistant to embolism yet vulnerable to irreversible hydraulic damage when it does occur (Johnson et al. 1999), typically maintain greater safety margins compared to woody angiosperms (Choat et al. 2012).

In contrast to pine, the oak species displayed responses to moderate drought stress indicative of anisohydric behavior, such as more negative water potential and maintenance of water use though the early phases of soil drying. These results are consistent with a large body of literature showing that

eastern U.S. oaks are less sensitive to declining soil moisture than co-occurring species (Meinzer et al. 2013, Thomsen et al. 2013, Roman et al. 2015, Matheny et al. 2017, Yi et al. 2019). Notably, these previous studies were conducted at drier sites to the south and west of our study site; thus, our results extend these findings to a cooler and more humid climate space.

When we examined J_s response below the threshold at which soil moisture becomes limiting for each species, we found strong control of J_s by VWC. The strength of the correlation between J_s and atmospheric controls (ET_0) below the breakpoint was significantly weaker than above the breakpoint for both species, reflecting a decoupling of stomatal regulation from atmospheric controls as soil moisture deficit increased. This decoupling effect was more pronounced for treatment trees compared to their counterpart control trees for both species, as we observed a lower correlation for treatment trees (R^2 = 0.40–0.45) than control trees (R^2 = 0.67–0.74). Similarly, a throughfall exclusion experiment in a 70-year old Ontario pine plantation also showed a marked switch between the primary controls on transpiration above (driven by VPD) and below (driven by soil moisture) the soil moisture threshold (MacKay et al. 2012). Nevertheless, both species in our study approached zero J_s at similar VWC thresholds (0.08–0.09 m^3m^{-3}), suggesting convergence of stomatal response under severe drought (e.g., Choat et al. 2012).

While white pine's high drought sensitivity was expected, the strong threshold behavior observed for the oaks deviates from much of the literature (discussed above). One possible explanation is that previous work mostly examined responses to relatively moderate natural droughts where minimum soil moisture didn't cross the thresholds we found. Of those studies that reported soil moisture data, minimum values ranged from 0.14 m^3m^{-3} at 10 cm depth (Roman et al. 2015) to 0.2 m^3m^{-3} between 0.1–0.5 m (Meinzer et al. 2013), compared to ~0.08 m^3m^{-3} between 10–30 cm depth in our treatment plot in 2016. Although soil VWC (integrated between 5 and 300 cm) reached 0.045 m^3m^{-3} in the study by Matheny et al., (2015), the authors attributed oaks' ability to continue transpiring under severe drought conditions to its deep rooting. While deep rooting is a trait often associated to oaks (Abrams et al. 1990), some studies suggest that oak species do not access as large of a soil water reservoir as co-occurring species (Roman et al. 2015, Berdanier and Clark 2018). In our study, although we cannot completely rule out the possibility that deep

rooting may have contributed to the oaks' relatively low initial sensitivity to declining soil moisture, the strong reduction in J_s in response to extremely low VWC suggests that even if our oaks are deeply rooted, they were unable to access sufficient water supplies during the peak of the 2016 drought.

The few studies that have examined effects of more severe droughts in the eastern U.S. suggest that oaks (and other ring porous and/or anisohydric species) may be more vulnerable to catastrophic damage to the hydraulic system during severe drought than co-occurring species (Hoffmann et al. 2011, Gu et al. 2015). For example, Hoffmann et al. (2011) found that 78% of stems among ring porous species exceeded 80 percent loss of xylem conductivity during a severe drought in the southeastern U.S., vs. only 44% of diffuse porous species stems. Although we did not directly measure changes in hydraulic conductivity, the lack of a rapid recovery of J_s after drought-breaking rains in September 2016 (Fig. 1) in the oak treatment trees (countered by the rapid recovery observed for all other trees), leads us to speculate that these trees experienced profound hydraulic dysfunction. Further, at the peak of the drought, treatment oaks maintained near-zero J_s for 26 days, compared to only 15 days of near-zero J_s in pine, consistent with the occurrence of hydraulic damage.

Two other studies have used experimental manipulations to assess drought response by temperate tree species in the eastern U.S. Wullschleger and Hanson (2006) conducted a 33% throughfall reduction experiment over 6 years in Oak Ridge, Tennessee, USA, and reported a 11 to 30% reduction in annual stand transpiration; however, no differences in individual species' growth responses to the TFE treatment were detected. In the second study, which involved a glasshouse experiment on saplings of dominant eastern tree species in Indiana, Kannenberg et al. (2019) reported that the anisohydric oaks experienced greater hydraulic damage but no significant C assimilation advantage compared to the more isohydric species. However, because saplings often respond differently to drought than mature trees (Cavender-Bares and Bazzaz 2000), and the experimental treatment created conditions of more rapid soil drying and lower plant water potential than most natural droughts (Kannenberg et al. 2019), the results are not directly comparable with our results for mature trees.

Recently, researchers have suggested that anisohydric species may shift towards more isohydric behavior (i.e. increased hydraulic safety margins) when soils become severely dry (Hochberg et al. 2018, Guo and Ogle 2019, Kannenberg et al. 2019, Guo et al. 2020), which could help avoid catastrophic damage to plant tissues. Following this line of reasoning, it is possible that both our control and treatment oak trees exhibited a shift towards more isohydric behavior. The inability of the treatment oaks to upregulate their J_s in response to the late 2016 rain event may indicate crossing of a critical threshold that exceeded their physiological capacity for short-term recovery (Zwieniecki and Secchi 2015). Similar to our control oak trees, Oren and Pataki (2001) observed an increase in J_s following rains occurring after a 13-day period without precipitation in white oak and attributed this to the recovery of hydraulic conductivity. Similarly, MacKay et al (2012) found that droughted pine trees quickly reached pre-drought transpiration levels once soil moisture levels increased. Additional data are needed to determine whether the lack of a recovery response in the treatment oaks' J_s to the drought-breaking rains may be attributed to catastrophic damage to their xylem tissue, a transitioning towards greater isohydric behavior and corresponding stomatal closure, or some other factor.

Response and recovery of woody stem growth

In our study, while both pine and oak experienced significant growth declines in response to the 2016 late season drought, the magnitude of the radial growth reduction was more than twice as great for pine (50% and 53% vs. 18% and 29% for control and treatment pines and oaks, respectively; Fig. 5). A regional-scale study that assessed woody stem growth response to drought among eastern U.S. tree species reported average growth declines ranging from 6.1–16.8% (D'Orangeville et al. 2018) for droughts with SPEI below -1.5. The greater growth declines found in our study may relate to the magnitude of the drought in this study (SPEI of -2.0 in control plots with stronger drought in the treatment plots), the greater sensitivity of species growing in the more humid NE, or both.

The sharply contrasting wood anatomies and growth phenologies of pine and oak may help explain their differing growth responses. As an evergreen species with embolism-resistant tracheid vascular

system, white pine typically begins photosynthesizing early in the growing season, with peak growth rates corresponding to the longest days in mid-June (Rossi et al. 2006), and growth often continues into late summer (Vose and Swank 1994, McIntire et al. 2020). In contrast, a large fraction of radial growth in oaks occurs during the early growing season and is completed by August (LeBlanc and Terrell 2009). Thus, we would expect the late season 2016 drought to have been more detrimental to pine's growth. Others have documented effects of late season droughts on white pine growth (Marchand and Filion 2012, Chhin et al. 2013, Livingston and Kenefic 2018). Pines' evergreen foliage may provide them with additional opportunities to replenish stored carbohydrates when oaks are fully dormant. Though most C fixed during the winter months may ultimately be used for respiration (Hansen et al. 1996, Sanders-DeMott et al. 2020), April is a time of reliably high soil moisture and fairly warm daytime temperatures but little or no active growth to serve as a C sink. The role of this time period in relieving past stress in white pine is worth investigating.

The large-diameter vessels characteristic of ring-porous oaks are highly vulnerable to cavitation during late season moisture deficit and winter freeze-thaw cycles; thus, oaks rely heavily on stored carbohydrates to produce early wood to reestablish their hydraulic conductive system and flush new leaves (Michelot et al. 2012, Pérez-de-Lis et al. 2017). Later in the growing season, oaks preferentially allocate carbohydrates to storage and less to growth (Hoch et al. 2003, Michelot et al. 2012, Bazot et al. 2013). Others have also documented relatively low growth sensitivity of oaks to current year drought (Klos et al. 2009, LeBlanc and Terrell 2011, Brzostek et al. 2014, Martin-Benito and Pederson 2015, Elliott et al. 2015).

The greater resistance of oak to the 2016 drought contrasts with the further growth declines the following year (i.e., low recovery), despite higher-than-average rainfall that resulted in soil moisture conditions in the treatment plots being close to normal. Indeed, several studies have reported a correlation between radial growth and prior-years late-season moisture in oak species (Orwig and Abrams 1997, Tardif et al. 2006, LeBlanc and Terrell 2011, Maxwell et al. 2015, D'Orangeville et al. 2018, Kannenberg et al. 2019). In contrast, pine showed either stable (treatment) or increasing (control) radial

growth in 2017. Similar to our study, Abrams et al. (2000) reported large growth declines in white pine in response to current-year drought, followed by growth release in response to favorable moisture conditions the following year. Conversely, Livingston and Kenefic (2018) documented continued growth declines in white pine following a late summer drought. Similarly, ring porous species were found to have much larger growth legacy effects compared to conifers (Kannenberg et al. 2019), and strongly anisohydric species with small safety margins often recover more slowly after severe drought (Brodribb and Cochard 2009, Anderegget al. 2015), potentially due to greater losses in hydraulic conductivity and repair needs (Skelton et al. 2015).

Stable C isotope ratios in tree rings, a metric of intrinsic water-use efficiency, show substantially greater iWUE for pine than for oaks, consistent with previous iWUE comparisons between conifers and deciduous angiosperms (Leavitt and Danzer 1993, Guerrieri et al. 2019, Vadeboncoeur et al. 2020) and between isohydric and anisohydric species (Cavender-Bares and Bazzaz, 2000). Time series of C-isotope discrimination were similar to those of annual wood growth observed for pine, with increased iWUE associated with growth reductions in 2016, and recovering to levels either lower (control trees) or slightly greater (treatment trees) than pre-treatment levels (Fig. 5). Other studies have also reported reductions in C-isotope discrimination in white pine during periods of drought (Leavitt 1993, McNulty and Swank 1995). This strong correlation of wood production and iWUE is indicative of an isohydric strategy by which stomatal conductance and C uptake are downregulated when soil conditions become moderately dry. In contrast to pine, only treatment oaks increased their iWUE during the drought, followed by full return to pre-treatment levels post-drought (Figs. 5-6), consistent with their lower soil moisture threshold for downregulating stomatal conductance. Similar to our findings, Yi et al. (2019) found that iWUE of isohydric species was more sensitive to changes in environmental conditions compared to anisohydric species.

In addition to the differences between pine and oak in isohydricity, wood structure, growth and foliar phenologies, and rooting habit (discussed above), they also exhibit other fundamentally different strategies that distinguish conifers from angiosperms. These include a suite of other coordinated traits

that support either an avoidant isohydric (pine) or tolerant anisohydric (oak) survival strategy for coping with environmental stress (Cailleret et al. 2019). While emerging theory suggests that drought-induced mortality may be triggered by different mechanisms for these two divergent strategies (i.e., referred to carbon starvation or hydraulic dysfunction), the role of stored non-structural carbohydrates in the refilling of embolized xylem tissue suggests a degree of interdependence between these two mortality pathways (Klein et al. 2018), while the precise mechanisms continue to be debated (Adams et al. 2017). Continued monitoring and additional measurements beyond the scope of this study are needed to address these questions.

Conclusions and future directions

In this study, we implemented a throughfall removal experiment to simulate a once-in-a-century drought, which coincided with the natural severe drought in 2016. Our results revealed clear differences in the sensitivity and threshold behavior of two dominant NE tree genera. The threshold that triggered an abrupt (nonlinear) reduction in transpiration occurred at a significantly higher soil VWC for pine compared to the oaks, suggesting that while threshold responses were observed for both species, pine was more sensitive to moderate drying. Growth declines were much more pronounced for the pines than the oaks; however, post-drought recovery of growth appears to be occurring more rapidly in the pine. Overall, our results lend support to the hypothesis that the oaks' anisohydric strategy may be most beneficial under moderate drought, but may result in greater vulnerability to extreme drought. This strategy may confer a competitive advantage over co-occurring species by enabling the oaks to maintain C uptake at the expense of greater risk of hydraulic damage in humid temperate environments where droughts have historically been infrequent and of moderate severity. Our findings extend previous analyses on drought effects on temperate tree species to include a simulated extreme drought in the NE USA. We note that our results are limited to contrasting *Pinus strobus* versus *Quercus rubra* and *Q. velutina,* which cannot fully represent these two highly diverse genera with broad geographic ranges, and that other *Pinus* and *Quercus* may have very different responses to drought (e.g., Steckel et al. 2020).

The critical role of soil moisture thresholds in determining oak resilience to drought also lend support to emerging evidence of major mortality events among *Lobatae* (red) oaks in response to past drought in the eastern U.S. (e.g. Druckenbrod et al. 2019). Our findings on species' differences in drought response have implications for advancing knowledge on the resilience and adaptive capacity of northeastern forests to future climate change.

Funding: This research was funded by the New Hampshire Agricultural Experiment Station (Accessions 1003450 and 1013351) and the Iola Hubbard Climate Endowment, managed by the Earth Systems Research Center at the University of New Hampshire. Views expressed in this paper are those of the authors and do not necessarily reflect those of the funding agencies. The use of trade names is for informational purposes only and does not imply endorsement.

Acknowledgements: We thank K. Vargas Moreno, V. García Peirotén, E. Perry, C. Twombly, R. Lafreneiere, T. Lindsay, K. Lavoie, R. Snyder, K. Accashian, C. Brenton, and K. Hammond for field and lab assistance. A. Ouimette conducted stable isotope analyses at the UNH Instrumentation Center. We thank J. Campbell, S. Eisenhaure, R. Guerrieri, L. Rustad, M. Smith, and the DroughtNet RCN (http://drought-net.colostate.edu) for contributions to study design. TFE plot infrastructure was fabricated by Verde Valley Construction LLC of Dover, NH. Thompson Farm is managed by the UNH Office of Woodlands and Natural Areas.

Cited References

Abrams MD, van de Gevel S, Dodson RC, Copenheaver CA (2000) The dendroecology and climatic impacts for old-growth white pine and hemlock on the extreme slopes of the Berkshire Hills, Massachusetts, U.S.A. Can J Bot 78:851–861.

Abrams MD, Schultz JC, Kleiner KW (1990) Ecophysiological responses in mesic versus xeric hardwood species to an early-season drought in central Pennsylvania. For Sci 36:970–981.

Adams HD, Zeppel MJB, Anderegg WRL, Hartmann H, Landhäusser SM, Tissue DT, Huxman TE, Hudson PJ, Franz TE, Allen CD, Anderegg LDL, Barron-Gafford GA, Beerling DJ, Breshears DD, Brodribb TJ, Bugmann H, Cobb RC, Collins AD, Dickman LT, Duan H, Ewers BE, Galiano L, Galvez DA, Garcia-Forner N, Gaylord ML, Germino MJ, Gessler A, Hacke UG, Hakamada R, Hector A, Jenkins MW, Kane JM, Kolb TE, Law DJ, Lewis JD, Limousin J-M, Love DM, Macalady AK, Martínez-Vilalta J, Mencuccini M, Mitchell PJ, Muss JD, O'Brien MJ, O'Grady AP, Pangle RE, Pinkard EA, Piper FI, Plaut JA, Pockman WT, Quirk J, Reinhardt K, Ripullone F, Ryan MG, Sala A, Sevanto S, Sperry JS, Vargas R, Vennetier M, Way DA, Xu C, Yepez EA, McDowell NG (2017) A multi-species synthesis of physiological mechanisms in drought-induced tree mortality. Nat Ecol Evol 1:1285–1291.

Allen CD, Macalady AK, Chenchouni H, Bachelet D, McDowell N, Vennetier M, Kitzberger T, Rigling A, Breshears DD, Hogg EH (Ted., Gonzalez P, Fensham R, Zhang Z, Castro J, Demidova N, Lim JH, Allard G, Running SW, Semerci A, Cobb N (2010) A global overview of drought and heat-induced tree mortality reveals emerging climate change risks for forests. For Ecol Manage 259:660–684.

Anderegg WRL, Flint A, Huang C, Flint L, Berry JA, Davis FW, Sperry JS, Field CB (2015) Tree mortality predicted from drought-induced vascular damage. Nat Geosci 8:367–371.

Anderegg WRL, Klein T, Bartlett M, Sack L, Pellegrini AFA, Choat B, Jansen S (2016) Meta-analysis reveals that hydraulic traits explain cross-species patterns of drought-induced tree mortality across the globe. Proc Natl Acad Sci 113:5024–5029.

Asbjornsen H, Campbell JL, Jennings KA, Vadeboncoeur MA, McIntire C, Templer PH, Phillips RP, Bauerle TL, Dietze MC, Frey SD, Groffman PM, Guerrieri R, Hanson PJ, Kelsey EP, Knapp AK, McDowell NG, Meir P, Novick KA, Ollinger S V, Pockman WT, Schaberg PG, Wullschleger SD, Smith MD, Rustad LE (2018) Guidelines and considerations for designing field experiments simulating precipitation extremes in forest ecosystems. Methods Ecol Evol 9:2310–2325.

Bazot S, Barthes L, Blanot D, Fresneau C (2013) Distribution of non-structural nitrogen and carbohydrate compounds in mature oak trees in a temperate forest at four key phenological stages. Trees - Struct Funct 27:1023–1034.

Beguería S, Latorre B, Reig F, Vicente-Serrano SM (2020) SPEI Global Drought Monitor. https://spei.csic.es/map/maps.html

Billings SA, Glaser SM, Boone AS, Stephen FM (2015) Nonlinear tree growth dynamics predict resilience to disturbance. Ecosphere 6:242.

Bovard BD, Curtis PS, Vogel CS, Su H-B, Schmid HP (2005) Environmental controls on sap flow in a northern hardwood forest. Tree Physiol 25:31–38.

Bowman DMJS, Brienen RJW, Gloor E, Phillips OL, Prior LD (2013) Detecting trends in tree growth: not so simple. Trends Plant Sci 18:11–17.

Brodribb TJ, Cochard H (2009) Hydraulic failure defines the recovery and point of death in water-stressed conifers. Plant Physiol 149:575–584.

Brzostek ER, Dragoni D, Schmid HP, Rahman AF, Sims D, Wayson CA, Johnson DJ, Phillips RP (2014) Chronic water stress reduces tree growth and the carbon sink of deciduous hardwood forests. Glob Chang Biol 20:2531–2539.

Burns RM, Honkala BH (1990) Silvics of North America. USDA Forest Service, Agriculture Handbook 654. https://srs.fs.usda.gov/pubs/11006

Cailleret M, Dakos V, Jansen S, Robert EMR, Aakala T, Amoroso MM, Antos JA, Bigler C, Bugmann H, Caccianaga M, Camarero J-J, Cherubini P, Coyea MR, Čufar K, Das AJ, Davi H, Gea-Izquierdo G, Gillner S, Haavik LJ, Hartmann H, Hereş A-M, Hultine KR, Janda P, Kane JM, Kharuk VI, Kitzberger T, Klein T, Levanic T, Linares J-C, Lombardi F, Mäkinen H, Mészáros I, Metsaranta JM, Oberhuber W, Papadopoulos A, Petritan AM, Rohner B, Sangüesa-Barreda G, Smith JM, Stan AB, Stojanovic DB, Suarez M-L, Svoboda M, Trotsiuk V, Villalba R, Westwood AR, Wyckoff PH, Martínez-Vilalta J (2019) Early-warning signals of individual tree mortality based on annual radial growth. Front Plant Sci 9:1964.

Camarero JJ, Gazol A, Sang G, Oliva J, Vicente-serrano SM (2015) To die or not to die: early warnings of tree dieback in response to a severe drought. J Ecol 103:44–57.

Cavin L, Mountford EP, Peterken GF, Jump AS (2013) Extreme drought alters competitive dominance within and between tree species in a mixed forest stand. Funct Ecol 27:1424–1435.

Chhin S, Chumack K, Dahl T, David ET, Kurzeja P, Magruder M, Telewski FW (2013) Growth-climate relationships of *Pinus strobus* in the floodway versus terrace forest along the banks of the Red Cedar River, Michigan. Tree-Ring Res 69:37–47.

Choat B, Jansen S, Brodribb TJ, Cochard H, Delzon S, Bhaskar R, Bucci SJ, Feild TS, Gleason SM, Hacke UG, Jacobsen AL, Lens F, Maherali H, Martínez-Vilalta J, Mayr S, Mencuccini M, Mitchell PJ, Nardini A, Pittermann J, Pratt RB, Sperry JS, Westoby M, Wright IJ, Zanne AE (2012) Global convergence in the vulnerability of forests to drought. Nature 491:752–755.

Coble AP, Contosta AR, Smith RG, Siegert NW, Vadeboncoeur M, Jennings KA, Stewart AJ, Asbjornsen H (2020) Influence of forest-to-silvopasture conversion and drought on components of evapotranspiration. Agric Ecosyst Environ 295:106916.

Coble AP, Vadeboncoeur MA, Berry ZC, Jennings KA, McIntire CD, Campbell JL, Rustad LE, Templer PH, Asbjornsen H (2017) Are Northeastern U.S. forests vulnerable to extreme drought? Ecol Process 6:34.

Cochard H, Tyree MT (1990) Xylem dysfunction in *Quercus*: vessel sizes, tyloses, cavitation and seasonal changes in embolism. Tree Physiol 6:393–407.

Cook ER, Pederson N (2011) Uncertainty, emergence, and statistics in dendroclimatology Hughes MK, Swetnam TW, Diaz HF (eds). Dev Paleoenviron Res 11:77–112.

D'Orangeville L, Maxwell J, Kneeshaw D, Pederson N, Duchesne L, Logan T, Houle D, Arseneault D, Beier CM, Bishop DA, Druckenbrod D, Fraver S, Girard F, Halman J, Hansen C, Hart JL, Hartmann H, Kaye M, Leblanc D, Manzoni S, Ouimet R, Rayback S, Rollinson CR, Phillips RP (2018) Drought timing and local climate determine the sensitivity of eastern temperate forests to drought. Glob Chang Biol 24:2339–2351.

Dai AG (2013) Increasing drought under global warming in observations and models. Nat Clim Chang 3:52–58.

Daly C, Halbleib M, Smith JI, Gibson WP, Doggett MK, Taylor GH, Curtis J, Pasteris PP (2008) Physiographically sensitive mapping of climatological temperature and precipitation across the conterminous United States. Int J Climatol 28:2031–2064.

De Grandpré L, Kneeshaw DD, Perigon S, Boucher D, Marchand M, Pureswaran D, Girardin MP (2019) Adverse climatic periods precede and amplify defoliator-induced tree mortality in eastern boreal North America. J Ecol 107:452–467.

DeSoto L, Cailleret M, Sterck F, Jansen S, Kramer K, Robert EMR, Aakala T, Amoroso MM, Bigler C, Camarero JJ, Čufar K, Gea-Izquierdo G, Gillner S, Haavik LJ, Hereş AM, Kane JM, Kharuk VI, Kitzberger T, Klein T, Levanič T, Linares JC, Mäkinen H, Oberhuber W, Papadopoulos A, Rohner B, Sangüesa-Barreda G, Stojanovic DB, Suárez ML, Villalba R, Martínez-Vilalta J (2020) Low growth resilience to drought is related to future mortality risk in trees. Nat Commun 11:1–9.

Dietze MC, Moorcroft PR (2011) Tree mortality in the eastern and central United States: Patterns and drivers. Glob Chang Biol 17:3312–3326.

Duchesne L, Houle D, Ouimet R, Caldwell L, Gloor M, Brienen R (2019) Large apparent growth increases in boreal forests inferred from tree-rings are an artefact of sampling biases. Sci Rep 9:6832.

Elliott KJ, Miniat CF, Pederson N, Laseter SH (2015) Forest tree growth response to hydroclimate variability in the southern Appalachians. Glob Chang Biol 21:4627–4641.

Farquhar GD, Ehleringer JR, Hubick KT (1989) Carbon isotope discrimination and photosynthesis. Annu Rev Plant Physiol Plant Mol Biol 40:503–537.

Federer CA (1980) Paper birch and white oak saplings differ in desponses to drought. For Sci 26:313–324.

Gu L, Pallardy SG, Hosman KP, Sun Y (2015) Drought-influenced mortality of tree species with different predawn leaf water dynamics in a decade-long study of a central US forest. Biogeosciences 12:2831–2845.

Guérin M, Martin-Benito D, von Arx G, Andreu-Hayles L, Griffin KL, Hamdan R, McDowell NG, Muscarella R, Pockman W, Gentine P (2018) Interannual variations in needle and sapwood traits of *Pinus edulis* branches under an experimental drought. Ecol Evol 8:1655–1672.

Guerrieri R, Belmecheri S, Ollinger S V., Asbjornsen H, Jennings K, Xiao J, Stocker BD, Martin M, Hollinger DY, Bracho-Garrillo R, Clark K, Dore S, Kolb T, Munger JW, Novick K, Richardson AD (2019) Disentangling the role of photosynthesis and stomatal conductance on rising forest water-use efficiency. Proc Natl Acad Sci 116:16909–16914.

Guo JS, Hultine KR, Koch GW, Kropp H, Ogle K (2020) Temporal shifts in iso/anisohydry revealed from daily observations of plant water potential in a dominant desert shrub. New Phytol 225:713–726.

Guo JS, Ogle K (2019) Antecedent soil water content and vapor pressure deficit interactively control water potential in *Larrea tridentata*. New Phytol 221:218–232.

Gustafson EJ, Sturtevant BR (2013) Modeling forest mortality caused by drought stress: implications for climate change. Ecosystems 16:60–74.

Hansen, J., Vogg, G., Beck, E., 1996. Assimilation, allocation and utilization of carbon by 3-year-old Scots pine (*Pinus sylvestris* L.) trees during winter and early spring. Trees - Struct. Funct. 11, 83–90.

Hipp AL, Manos PS, González-Rodríguez A, Hahn M, Kaproth M, McVay JD, Avalos SV, Cavender-Bares J (2018) Sympatric parallel diversification of major oak clades in the Americas and the origins of Mexican species diversity. New Phytol 217:439–452.

Hoch G, Richter A, Korner C (2003) Non-structural carbon compounds in temperate forest trees. Plant, Cell Environ 26:1067–1081.

Hochberg U, Rockwell FE, Holbrook NM, Cochard H (2018) Iso/Anisohydry: A Plant–Environment Interaction Rather Than a Simple Hydraulic Trait. Trends Plant Sci 23:112–120.

Hoffmann WA, Marchin RM, Abit P, Lau OL (2011) Hydraulic failure and tree dieback are associated with high wood density in a temperate forest under extreme drought. Glob Chang Biol 17:2731–2742.

Huntington TG, Richardson AD, McGuire KJ, Hayhoe K (2009) Climate and hydrological changes in the northeastern United States: recent trends and implications for forested and aquatic ecosystems. Can J For Res 39:199–212.

Irvine J, Perks MP, Magnani F, Grace J (1998) The response of *Pinus sylvestris* to drought: Stomatal control of transpiration and hydraulic conductance. Tree Physiol 18:393–402.

Isaac-Renton M, Montwé D, Hamann A, Spiecker H, Cherubini P, Treydte K (2018) Northern forest tree populations are physiologically maladapted to drought. Nat Commun 9:5254.

Johnson NC, O'Dell TE, Bledsoe CS (1999) Methods for ecological studies of mycorrhizae. In: Standard Soil Methods for Long-term Ecological Research.pp 378–412.

Kannenberg SA, Novick KA, Phillips RP (2019) Anisohydric behavior linked to persistent hydraulic damage and delayed drought recovery across seven North American tree species. New Phytol 222:1862–1872.

Katabuchi M (2015) LeafArea: an R package for rapid digital image analysis of leaf area. Ecol Res 30:1073–1077.

Klein T (2014) The variability of stomatal sensitivity to leaf water potential across tree species indicates a continuum between isohydric and anisohydric behaviours. Funct Ecol 28:1313–1320.

Klein T, Zeppel MJB, Anderegg WRL, Bloemen J, De Kauwe MG, Hudson P, Ruehr NK, Powell TL, von Arx G, Nardini A (2018) Xylem embolism refilling and resilience against drought-induced mortality in woody plants: processes and trade-offs. Ecol Res 33:839–855.

Klos RJ, Wang GG, Bauerle WL, Rieck JR (2009) Drought impact on forest growth and mortality in the southeast USA: an analysis using Forest Health and Monitoring data. Ecol Appl 19:699–708.

Knapp AK, Avolio ML, Beier C, Carroll CJW, Collins SL, Dukes JS, Fraser LH, Griffin-Nolan RJ, Hoover DL, Jentsch A, Loik ME, Phillips RP, Post AK, Sala OE, Slette IJ, Yahdjian L, Smith MD (2017) Pushing precipitation to the extremes in distributed experiments: recommendations for simulating wet and dry years. Glob Chang Biol 23:1774–1782.

Krakauer NY, Lakhankar T (2019) Trends in drought over the northeast United States. Water 11:1834.

Kubiske ME, Abrams MD (1994) Ecophysiological analysis of woody species in contrasting temperate communities during wet and dry years. Oecologia 98:303–312.

Leavitt SW (1993) Seasonal $^{13}C/^{12}C$ changes in tree rings: species and site coherence, and a possible drought influence. Can J For Res 23:210–218.

Leavitt SW, Danzer SR (1993) Method for batch processing small wood samples to holocellulose for stable-carbon isotope analysis. Anal Chem 65:87–89.

LeBlanc DC, Berland AM (2019) Spatial variation in oak (*Quercus* spp.) radial growth responses to drought stress in eastern North America. Can J For Res 49:986–993.

LeBlanc DC, Terrell MA (2009) Radial growth response of white oak to climate in eastern North America. Can J For Res 39:2180–2192.

LeBlanc DC, Terrell MA (2011) Comparison of growth-climate relationships between northern red oak and white oak across eastern North America. Can J For Res 41:1936–1947.

Livingston WH, Kenefic LS (2018) Low densities in white pine stands reduce risk of drought-incited decline. For Ecol Manage 423:84–93.

MacKay SL, Arain MA, Khomik M, Brodeur JJ, Schumacher J, Hartmann H, Peichl M (2012) The impact of induced drought on transpiration and growth in a temperate pine plantation forest. Hydrol Process 26:1779–1791.

Maherali H, Moura CF, Caldeira MC, Willson CJ, Jackson RB (2006) Functional coordination between leaf gas exchange and vulnerability to xylem cavitation in temperate forest trees. Plant, Cell Environ 29:571–583.

Mamet SD, Chun KP, Metsaranta JM, Barr AG, Johnstone JF (2015) Tree rings provide early warning signals of jack pine mortality across a moisture gradient in the southern boreal forest. Environ Res Lett 10:084021.

Marchand N, Filion L (2012) False rings in the white pine (*Pinus strobus*) of the Outaouais Hills, Québec (Canada), as indicators of water stress. Can J For Res 42:12–22.

Martin-Benito D, Pederson N (2015) Convergence in drought stress, but a divergence of climatic drivers across a latitudinal gradient in a temperate broadleaf forest. J Biogeogr 42:925–937.

Martin P, Newton AC, Cantarello E, Evans PM (2017) Analysis of ecological thresholds in a temperate forest undergoing dieback Gomory D (ed). PLoS One 12:e0189578.

Matheny AM, Bohrer G, Garrity SR, Morin TH, Howard CJ, Vogel CS (2015) Observations of stem water storage in trees of opposing hydraulic strategies. Ecosphere 6:165.

Matheny AM, Fiorella RP, Bohrer G, Poulsen CJ, Morin TH, Wunderlich A, Vogel CS, Curtis PS (2017) Contrasting strategies of hydraulic control in two codominant temperate tree species. Ecohydrology 10:e1815.

Mathias JM, Thomas RB (2018) Disentangling the effects of acidic air pollution, atmospheric CO_2, and climate change on recent growth of red spruce trees in the Central Appalachian Mountains. Glob Chang Biol 24:3938–3953.

Mauna Loa Sampling Station Record (2018) Scripps CO_2 Progr. http://scrippsco2.ucsd.edu/data/atmospheric_co2/mlo

Maxwell JT, Harley GL, Matheus TJ (2015) Dendroclimatic reconstructions from multiple co-occurring species: A case study from an old-growth deciduous forest in Indiana, USA. Int J Climatol 35:860–870.

McCarroll D, Loader NJ (2004) Stable isotopes in tree rings. Quat Sci Rev 23:771–801.

McDowell NG, Fisher RA, Xu C, Domec JC, Hölttä T, Mackay DS, Sperry JS, Boutz A, Dickman L, Gehres N, Limousin JM, Macalady A, Martínez-Vilalta J, Mencuccini M, Plaut JA, Ogée J, Pangle RE, Rasse DP, Ryan MG, Sevanto S, Waring RH, Williams AP, Yepez EA, Pockman WT (2013) Evaluating theories of drought-induced vegetation mortality using a multimodel-experiment framework. New Phytol 200:304–321.

McDowell N, Pockman WT, Allen CD, Breshears DD, Cobb N, Kolb T, Plaut J, Sperry J, West A, Williams DG, Yepez EA (2008) Mechanisms of plant survival and mortality during drought: why do some plants survive while others succumb to drought? New Phytol 178:719–739.

McIntire CD, Huggett BA, Dunn E, Munck IA, Vadeboncoeur MA, Asbjornsen H (2020) Pathogen-induced defoliation impacts on transpiration, leaf gas exchange, and non-structural carbohydrate allocation in eastern white pine (*Pinus strobus*). Trees - Struct Funct, in press

McNulty SG, Swank WT (1995) Wood $\delta^{13}C$ as a measure of annual basal area growth and soil water stress in a *Pinus strobus* forest. Ecology 76:1581–1586.

Meinzer FC, Woodruff DR, Eissenstat DM, Lin HS, Adams TS, McCulloh KA (2013) Above-and belowground controls on water use by trees of different wood types in an eastern US deciduous forest. Tree Physiol 33:345–356.

Meir P, Wood TE, Galbraith DR, Brando PM, Da Costa ACL, Rowland L, Ferreira L V (2015) Threshold responses to aoil moisture deficit by trees and soil in tropical rain forests: Insights from field experiments. Bioscience 65:882–892.

Michelot A, Simard S, Rathgeber C, Dufrene E, Damesin C (2012) Comparing the intra-annual wood formation of three European species (*Fagus sylvatica*, *Quercus petraea* and *Pinus sylvestris*) as related to leaf phenology and non-structural carbohydrate dynamics. Tree Physiol 32:1033–1045.

Mitchell PJ, O'Grady AP, Hayes KR, Pinkard EA (2014) Exposure of trees to drought-induced die-off is defined by a common climatic threshold across different vegetation types. Ecol Evol 4:1088–1101.

Mitchell PJ, O'Grady AP, Pinkard EA, Brodribb TJ, Arndt SK, Blackman CJ, Duursma RA, Fensham RJ, Hilbert DW, Nitschke CR, Norris J, Roxburgh SH, Ruthrof KX, Tissue DT (2016) An ecoclimatic framework for evaluating the resilience of vegetation to water deficit. Glob Chang Biol 22:1677–1689.

Muggeo VMR (2008) Segmented : An R package to fit regression models with broken-line relationships. R News 8:25–30.

Niinemets Ü, Valladares F (2006) Tolerance to shade, drought, and waterlogging of temperate northern hemisphere trees and shrubs. Ecol Monogr 76:521–547.

Olson M, Rosell JA, Martínez-Pérez C, León-Gómez C, Fajardo A, Isnard S, Cervantes-Alcayde MA, Echeverría A, Figueroa-Abundiz VA, Segovia-Rivas A, Trueba S, Vázquez-Segovia K (2020) Xylem vessel-diameter–shoot-length scaling: ecological significance of porosity types and other traits. Ecol Monogr 90: e01410.

Oren R, Pataki DE (2001) Transpiration in response to variation in microclimate and soil moisture in southeastern deciduous forests. Oecologia 127:549–559.

Oren R, Sperry JS, Katul GG, Pataki DE, Ewers BE, Phillips N, Schäfer KVR (1999) Survey and synthesis of intra- and interspecific variation in stomatal sensitivity to vapour pressure deficit. Plant Cell Environ 22:1515–1526.

Orwig DA, Abrams MD (1997) Variation in radial growth responses to drought among species, site, and canopy strata. Trees - Struct Funct 11:474–484.

Pangle RE, Hill JP, Plaut JA, Yepez EA, Elliot JR, Gehres N, McDowell NG, Pockman WT (2012) Methodology and performance of a rainfall manipulation experiment in a piñon–juniper woodland. Ecosphere 3:art28.

Pederson N, Dyer JM, McEwan RW, Hessl AE, Mock CJ, Orwig DA, Rieder HE, Cook BI (2014) The legacy of episodic climatic events in shaping temperate, broadleaf forests. Ecol Monogr 84:599–620.

Pérez-de-Lis G, Olano JM, Rozas V, Rossi S, Vázquez-Ruiz RA, García-González I (2017) Environmental conditions and vascular cambium regulate carbon allocation to xylem growth in deciduous oaks. Funct Ecol 31:592–603.

Peters MP, Iverson LR, Matthews SN (2015) Long-term droughtiness and drought tolerance of eastern US forests over five decades. For Ecol Manage 345:56–64.

Plaut JA, Yepez EA, Hill J, Pangle R, Sperry JS, Pockman WT, McDowell NG (2012) Hydraulic limits preceding mortality in a piñon-juniper woodland under experimental drought. Plant, Cell Environ 35:1601–17.

R Core Team (2017) R: A Language and Environment for Statistical Computing.

Roman DT, Novick KA, Brzostek ER, Dragoni D, Rahman F, Phillips RP (2015) The role of isohydric and anisohydric species in determining ecosystem-scale response to severe drought. Oecologia 179:641–654.

Rossi S, Deslauriers A, Anfodillo T, Morin H, Saracino A, Motta R, Borghetti M (2006) Conifers in cold environments synchronize maximum growth rate of tree-ring formation with day length. New Phytol 170:301–310.

Sánchez-Costa E, Poyatos R, Sabaté S (2015) Contrasting growth and water use strategies in four co-occurring Mediterranean tree species revealed by concurrent measurements of sap flow and stem diameter variations. Agric For Meteorol 207:24–37.

Sánchez-Salguero R, Colangelo M, Matías L, Ripullone F, Camarero JJ (2020) Shifts in growth responses to climate and exceeded drought-vulnerability thresholds characterize dieback in two Mediterranean deciduous oaks. Forests 11:714.

Sanders-DeMott R, Ouimette AP, Lepine LC, Fogarty SZ, Burakowski EA, Contosta AR, Ollinger SV (2020) Divergent carbon cycle response of forest and grass-dominated northern temperate ecosystems to record winter warming. Glob Chang Biol 26: 1519-1531.

Skelton RP, West AG, Dawson TE (2015) Predicting plant vulnerability to drought in biodiverse regions using functional traits. Proc Natl Acad Sci 112:5744–5749.

Speer JH (2010) Fundamentals of Tree-Ring Research. The University of Arizona Press, Tucson, AZ.

Steckel M, del Río M, Heym M, Aldea J, Bielak K, Brazaitis G, Černý J, Coll L, Collet C, Ehbrecht M, Jansons A, Nothdurft A, Pach M, Pardos M, Ponette Q, Reventlow DOJ, Sitko R, Svoboda M, Vallet P, Wolff B, Pretzsch H (2020) Species mixing reduces drought susceptibility of Scots pine (*Pinus sylvestris* L.) and oak (*Quercus robur* L., *Quercus petraea* (Matt.) Liebl.) – Site water supply and fertility modify the mixing effect. For. Ecol. Manage. 461, 117908.

Sweet SK, Wolfe DW, Degaetano A, Benner R (2017) Anatomy of the 2016 drought in the Northeastern United States: Implications for agriculture and water resources in humid climates. Agric For Meteorol 247:571–581.

Tardif JC, Conciatori F, Nantel P, Gagnon D (2006) Radial growth and climate responses of white oak (*Quercus alba*) and northern red oak (*Quercus rubra*) at the northern distribution limit of white oak in Quebec, Canada. J Biogeogr 33:1657–1669.

Thomsen J, Bohrer G, Matheny A, Ivanov V, He L, Renninger H, Schäfer K (2013) Contrasting hydraulic strategies during dry soil conditions in *Quercus rubra* and *Acer rubrum* in a sandy site in Michigan. Forests 4:1106–1120.

US Drought Monitor (2020) New Hampshire Drought Monitor. https://droughtmonitor.unl.edu/

Vadeboncoeur MA, Jennings KA, Ouimette AP, Asbjornsen H (2020) Correcting tree-ring $\delta^{13}C$ time series for tree-size effects in eight temperate tree species. Tree Physiol 40:333–349.

Venturas MD, MacKinnon ED, Jacobsen AL, Pratt RB (2015) Excising stem samples underwater at native tension does not induce xylem cavitation. Plant Cell Environ 38:1060–1068.

Vose JM, Swank WT (1994) Effects of long-term drought on the hydrology and growth of a white pine plantation in the southern Appalachians. For Ecol Manage 64:25–39.

Wubbels JK (2010) Tree species distribution in relation to stem hydraulic traits and soil moisture in a mixed hardwood forest in central Pennsylvania. MSc Thesis, The Pennsylvania State University. https://criticalzone.org/shale-hills/publications/pub/wubbles-2010-tree-species-distribution-in-relation-to-stem-hydraulic-traits/

Xiao J, Zhuang Q, Law BE, Baldocchi DD, Chen J, Richardson AD, Melillo JM, Davis KJ, Hollinger DY, Wharton S, Oren R, Noormets A, Fischer ML, Verma SB, Cook DR, Sun G, McNulty S, Wofsy SC, Bolstad P V., Burns SP, Curtis PS, Drake BG, Falk M, Foster DR, Gu L, Hadley JL, Katul GG, Litvak M, Ma S, Martin TA, Matamala R, Meyers TP, Monson RK, Munger JW, Oechel WC, Paw UKT, Schmid HP, Scott RL, Starr G, Suyker AE, Torn MS (2011) Assessing net ecosystem carbon exchange of U.S. terrestrial ecosystems by integrating eddy covariance flux measurements and satellite observations. Agric For Meteorol 151:60–69.

Yi K, Dragoni D, Phillips RP, Roman DT, Novick KA (2017) Dynamics of stem water uptake among isohydric and anisohydric species experiencing a severe drought Phillips N (ed). Tree Physiol 37:1379–1392.

Yi K, Maxwell JT, Wenzel MK, Roman DT, Sauer PE, Phillips RP, Novick KA (2019) Linking variation in intrinsic water-use efficiency to isohydricity: a comparison at multiple spatiotemporal scales. New Phytol 221:195–208.

Zotarelli L, Dukes MD, Romero CC, Migliaccio KW, Morga KT (2010) Step by step calculation of the Penman-Monteith Evapotranspiration (FAO-56 Method). University of Florida, IFAS Extension. https://edis.ifas.ufl.edu/pdffiles/AE/AE45900.pdf

Zwieniecki MA, Secchi F (2015) Threats to xylem hydraulic function of trees under 'new climate normal' conditions. Plant Cell Environ 38:1713–1724.

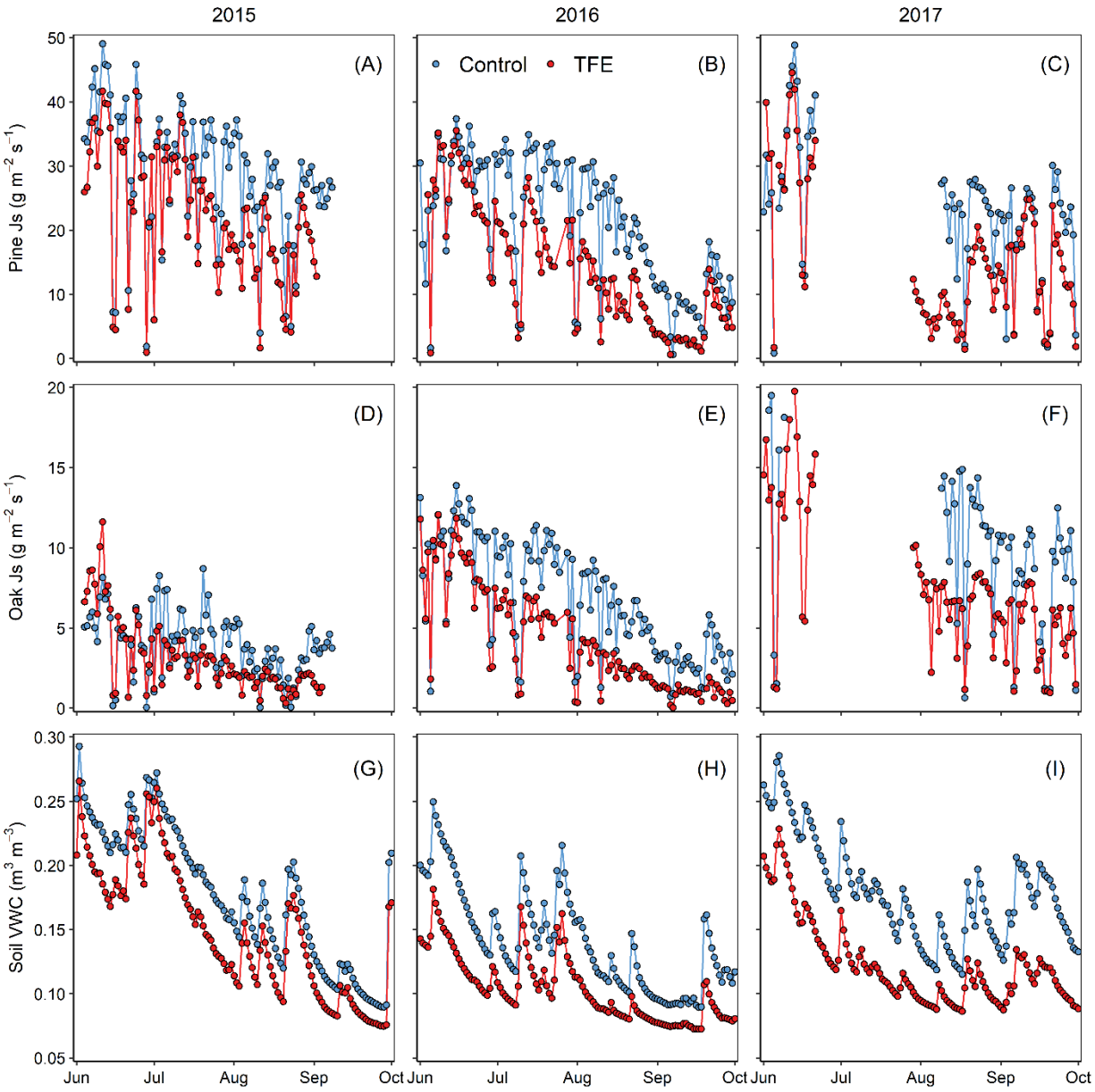

Figure 1. Mean daily sap flux density (J_s) for pines (A-C), and oaks (D-F) each year, panels correspond to 2015, 2016, and 2017 from left to right. Note the difference in y-axis scale for J_s between the two species. Soil volumetric water content (VWC, 10–30cm depth integrated mean) are shown for comparison in panels G-I). Blue represents control plots and red represents throughfall exclusion plots.

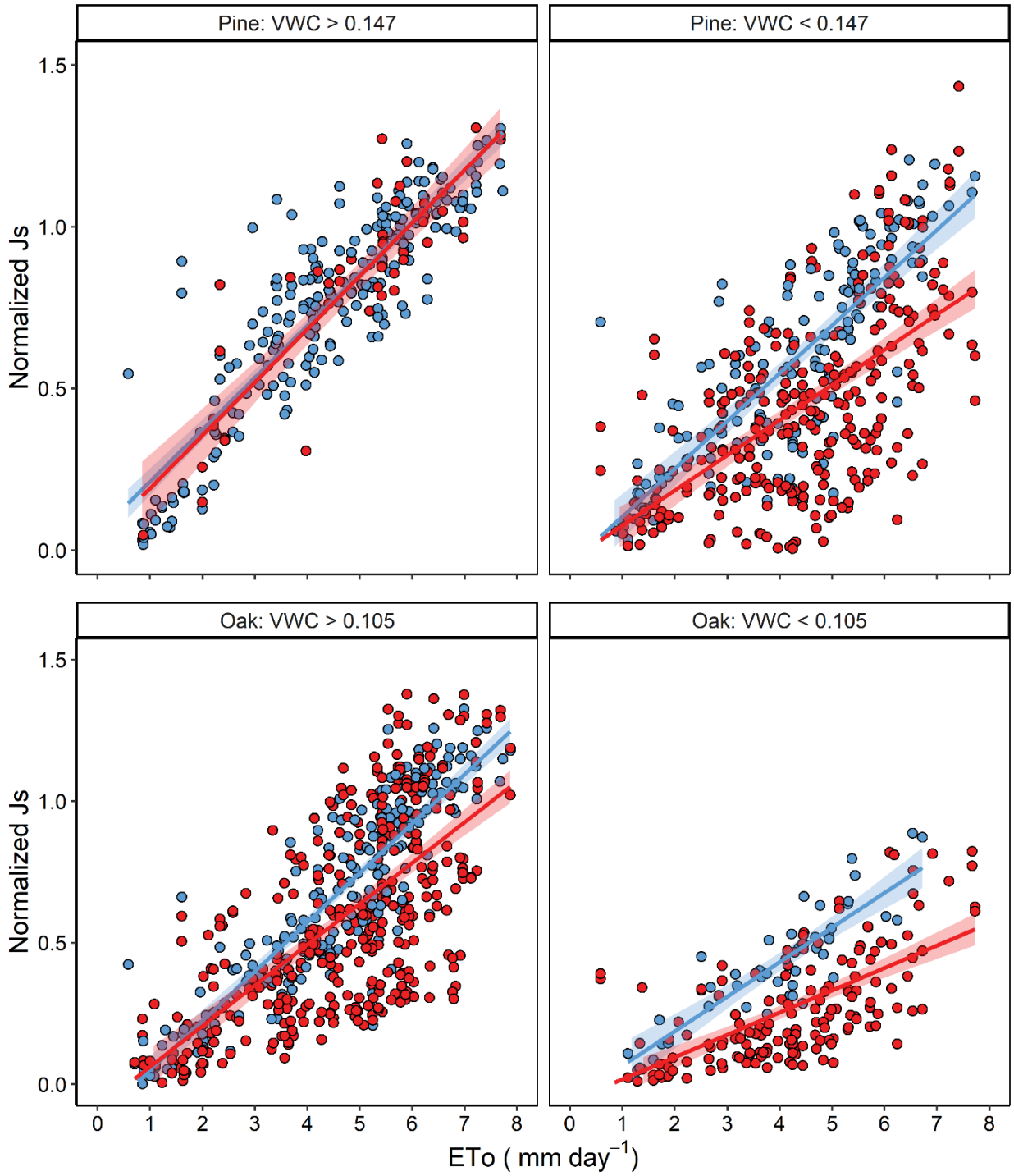

Figure 2. Mean daily sap flux density (J_s) as a function of the mean daily integrated (10–30 cm) soil volumetric water content ($m^3\ m^{-3}$). Each point represents the mean of trees per control (blue) and throughfall exclusion (red) for *P. strobus* (top; n = 6 trees per treatment) and *Quercus* (bottom; n = 3 trees for control, n = 6 for drought). Linear fits are shown with 95% CI (shaded).

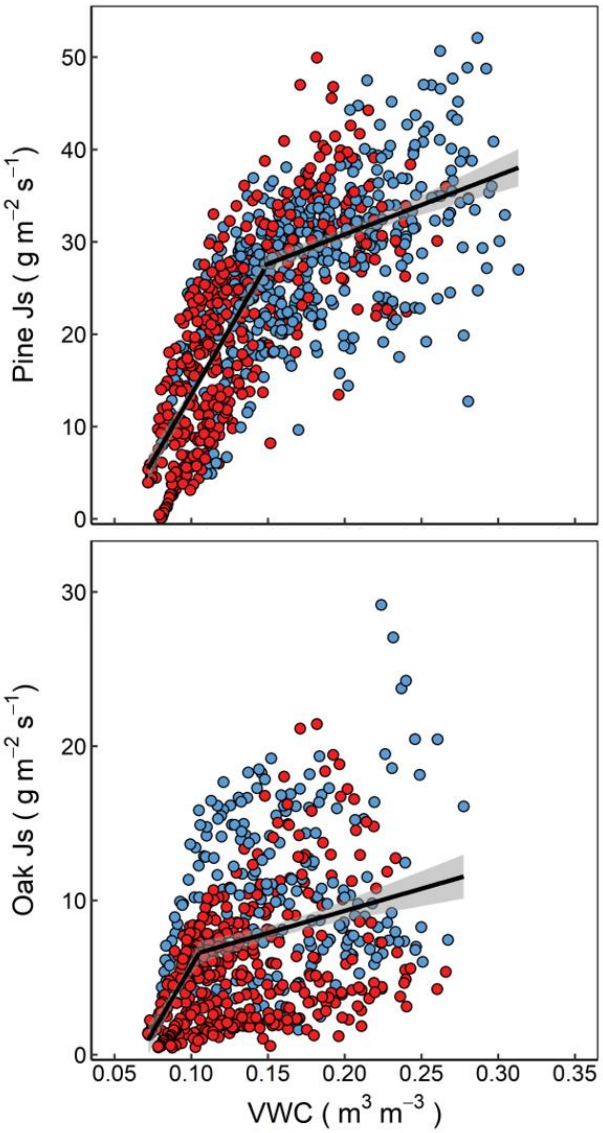

Figure 3. Mean daily sap flux density (J_s) normalized by the mean June Js for within each treatment year (2016 and 2017) as a function of daily reference evapotranspiration (ET_0) for trees within control (blue) and throughfall exclusion treatment (red) plots. Shaded regions of regression fits show the 95% confidence interval. Top and bottom panels show fits for *Pinus strobus* and *Quercus* respectively. Left and right panels show the upper and lower end of the VWC break point values respectively.

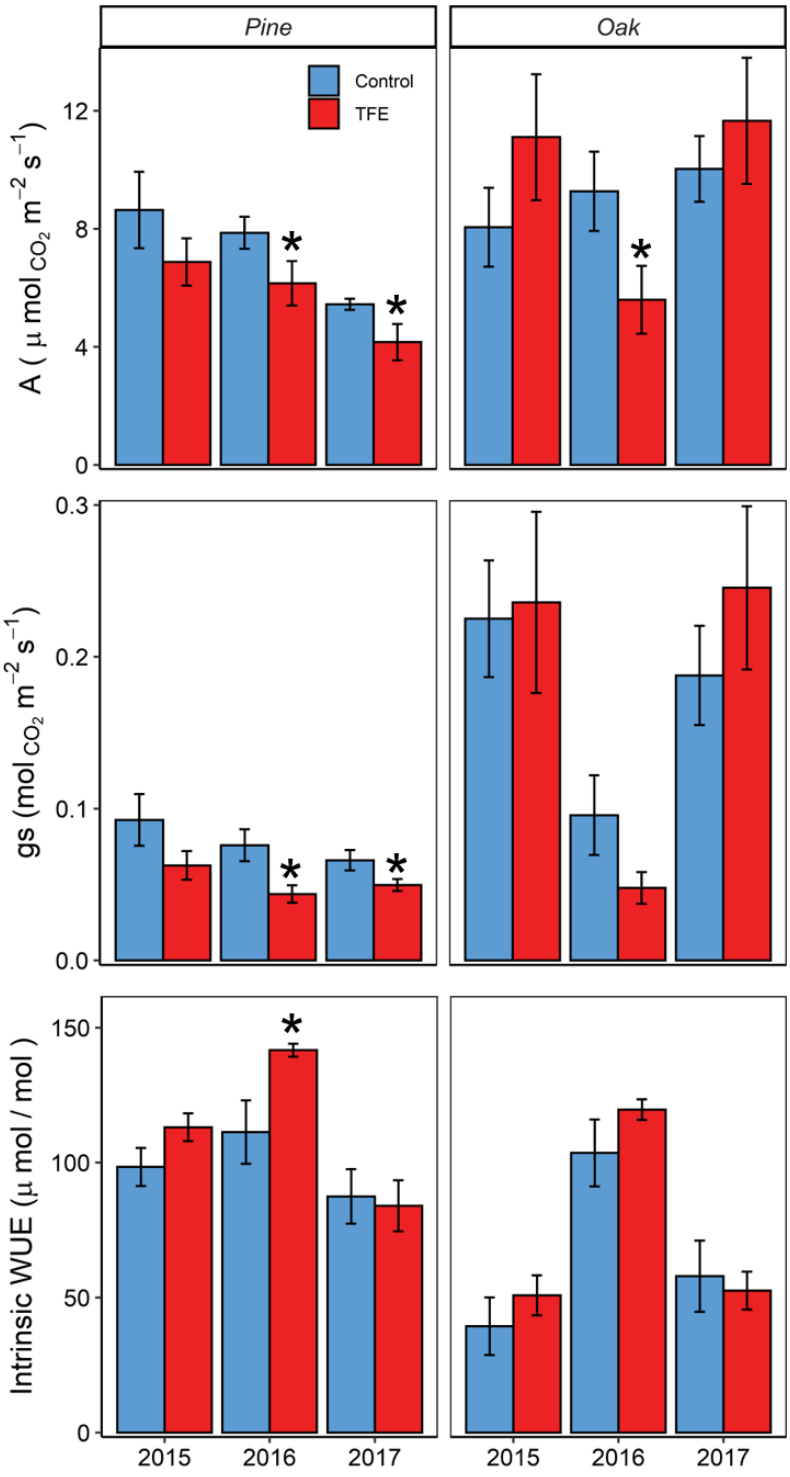

Figure 4. Leaf gas exchange measured in August of each year for control (blue) and throughfall exclusion (red) plots, error bars show standard error. * symbols denote significant difference ($p < 0.05$) via a one-tailed *t*-test in the post-treatment years 2016 and 2017.

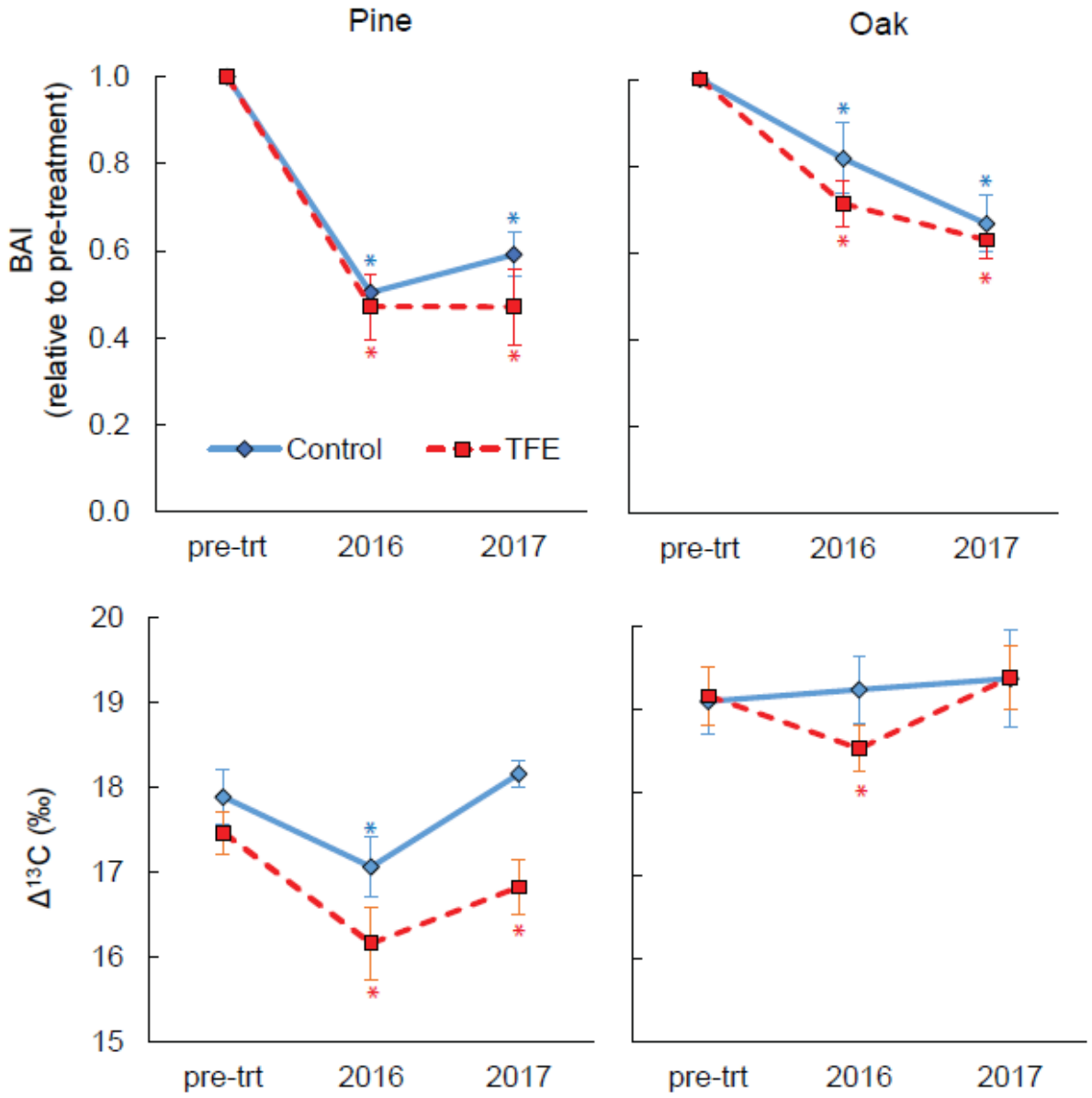

Figure 5. Basal area increment (BAI) and ^{13}C discrimination (Δ) from tree ring samples (lower values correspond with lower c_i/c_a ratios and higher intrinsic water use efficiency). Error bars show 1 SE. Blue and red asterisks indicate a significant difference from the pre-treatment period (2011-15) within a treatment.

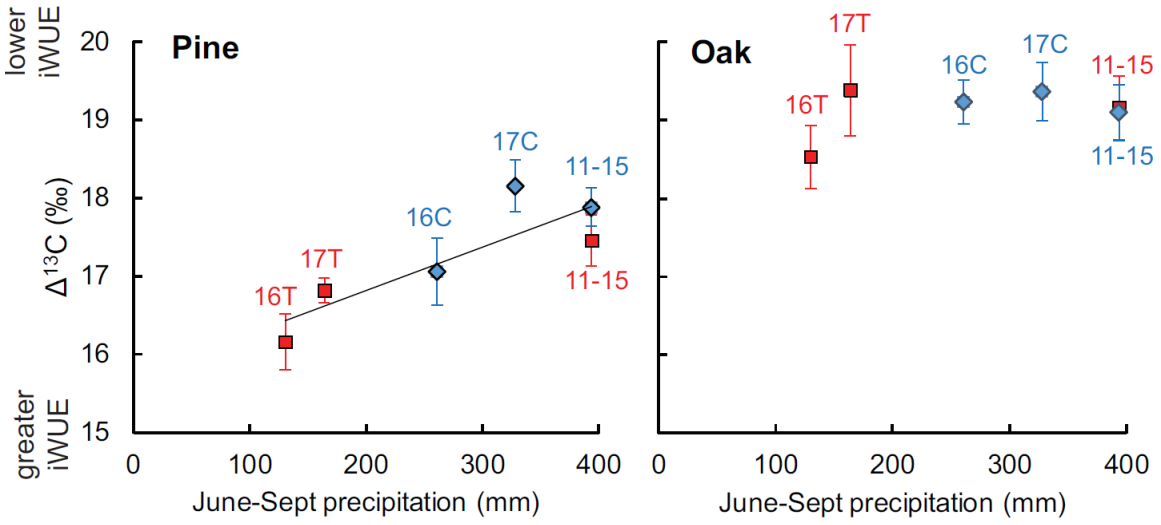

Figure 6. Relationship between ^{13}C discrimination (Δ) and growing season precipitation. In the post-treatment years, precipitation in the treatment plots is estimated as 50% of ambient (see Supplement 1a). Red squares are throughfall exclusion treatment trees and blue diamonds are control trees. The highest precipitation value represents the pre-treatment period (2011-15), and the lowest values within each treatment are 2016. The linear regression is significant for pine ($p = 0.02$; $R^2 = 0.74$), but there is not a significant linear relationship for oak. The 30-year mean June-September precipitation (for 1981-2010; PRISM) is 384 mm.

Supplementary Material

for:

H. Asbjornsen, C.D. McIntire, M.A. Vadeboncoeur, K.A. Jennings, A.P. Coble, and Z.C. Berry

Sensitivity and threshold dynamics of *Pinus strobus* and *Quercus spp.* in response to experimental and naturally-occurring severe droughts

Tree Physiology, 2021

Contents:

Supplement 1: Supplemental Methods

S1a: Estimation of Throughfall Removal

The throughfall removal structure design specification of 55% area coverage was based on an estimate that 51.6% precipitation removal would be required to achieve a 1-in-100 year drought event based on the historic record (1900-2014 PRISM data; see Knapp et al., 2015), while allowing for stemflow estimated at 3.2%, the mean of published values for *Q. rubra* (4%; Durocher, 1990) and *P. strobus* (2.3%; Helvey, 1967). The actual measured plastic coverage of the structures as built is 57.0% at plot T1 and 54.7% at plot T2. Visual estimates of leaks and litter-dam spillover observed during moderate to heavy rain events average in the range of 5 – 10% of total intercepted volume. Litter dams are regularly cleared from the troughs and gutters, and leaks are flagged for repair under dry conditions.

To characterize the magnitude of our throughfall removal treatment relative to interannual variation in precipitation (Fig S2) and to relate seasonally integrated iWUE to precipitation on a treatment-by-year basis (Fig 6), we estimated the effectiveness of throughfall removal as follows:

We start by ignoring any water retained by the canopy which ultimately evaporates rather than dripping, as this water is unavailable to roots and should not vary between treatment and control plots. We then assume that 3.2% of the remaining precipitation bypasses the structure as stemflow. If 55.8% (average plastic coverage area) of the remaining 96.8% (i.e. throughfall) is intercepted by the TFE structure, that means 54.0% of total soil-destined precipitation is intercepted. If 90 – 95% of this amount is successfully diverted off-plot rather than leaked within the plot, then our effective diversion of total soil-destined precipitation would be 48.6 – 51.3%. Realistically, there is an error range of several percentage points on each of the components in this calculation, but a nominal value of 50% meets our heuristic needs.

S1b: Sap Flow Measurements and Analysis

Our sap flow methodology employed the heat-ratio method (HRM), a heat-pulse based sap flow measurement technique that is excellent at resolving low flows and sap velocities up to approximately 50 cm h^{-1} (Burgess et al., 2001; Steppe et al., 2010). Sap flow probes were constructed at the University of New Hampshire using a protocol adapted from Davis et al., (2012). Probes contained three type-T thermocouple junctions along the length of a 1.0 mm diameter steel needle, allowing for temperature measurements at depths of 10, 22, and 35 mm into the sapwood. Prior to installation, bark and cambial tissue was carefully removed from the measurement point to ensure probes were in direct contact with the xylem. A metal drill guide was placed onto the exposed area allowing for accurate spacing between sensor probes and proper vertical alignment. Thermocouple probes were coated in petroleum jelly and positioned at a distance 0.6 cm up- and downstream of a 37 mm nichrome line heater (17–20 Ω), installed radially into the sapwood. Reflective closed-cell insulation was placed over the sensors to limit heating via direct sunlight. Sensors were connected to a datalogger and multiplexor (CR1000 and AM16/32; Campbell Scientific Inc., Logan, UT, USA) powered by an external 12 V battery. A heat pulse of 2.5 s duration was generated by each heating probe on a 15-min interval and the change in temperature 60-100 s following the heat pulse was recorded for the up- and downstream thermocouples.

After processing the 2015 data, we decided to optimize the sensor design for oaks with shallower sensor depths in 2016, because oaks have narrow functional sapwood and typically show little or no sap flow beyond 2 cm depth (see also Berdanier et al., 2016; Miller et al., 1980; Poyatos et al., 2007; Renninger and Schäfer, 2012; Yi et al., 2017). Mean sapwood depth among oaks measured in this study was 23.1 mm (SE ± 2.2). These optimized oak sap flow sensors had thermocouples at depths of 5, 10, and 15 mm from the cambium, and were used in 2016–2017. To better compare data across years, we scaled the data from the 10 mm depth in 2015 to estimate sap velocities at the 5 mm depth and did not use data from the 35 mm depth (Fig. S2).

The total sapwood area for each target tree was estimated from increment core samples collected from each target tree in 2015. To limit repeated destructive sampling of target trees in subsequent years, sapwood density (ρ_d) and moisture content (m_c) was determined gravimetrically for each tree from increment core samples collected off-plot from n=10 trees of each species. Similar samples were also collected at four different times throughout the 2014 growing season in order to provide a robust seasonal average for each species. Sapwood thermal diffusivity (D) was calculated according to (Vandegehuchte and Steppe, 2013), for which we report a mean value of 0.0023 $cm^2\ s^{-1}$ and 0.0027 $cm^2\ s^{-1}$ for white pine and red oak respectively, a value close to the nominal value of 0.0025 $cm^2\ s^{-1}$ that is often used across HRM studies (Looker et al., 2016; Marshall, 1958). The heat pulse velocity (V_h) is calculated as described by (McIntire et al., in press), applying the standard equations and corrections as suggested in (Burgess et al., 2001). The heat pulse velocity (V_h) is calculated as:

$$V_h = \frac{D}{x} ln\left(\frac{v_1}{v_2}\right) 3600$$

Where x is the distance of from the heat source (cm), and v_1 and v_2 are the changes in temperature (°C) of the upstream and downstream thermocouples, respectively. Using the methodology of Burgess et al. (2001), corrections to V_h for probe misalignment and wounding were conducted. Zero-flow conditions are often determined using low vapor pressure deficit (VPD) at night and/or periods of 100% relative humidity during the day (Ambrose et al., 2010; Gotsch et al., 2014). Following determination of V_h zero flow, sap flux density is then calculated as:

$$J_s = \frac{\rho_d}{\rho_s}\left(m_c + \frac{c_{dw}}{c_s}\right) V_h$$

Where J_s is the sap flux density ($cm^3\ cm^{-2}\ h^{-1}$), ρ_s is the density of sap (1000 kg m^{-3}) c_{dw} is the specific heat capacity of the wood matrix (1200 J $kg^{-1}\ K^{-1}$), and c_s is the heat capacity of water (4186 J $kg^{-1}\ K^{-1}$). As Js is known to decline from the outer xylem towards the sapwood, the radial profile must be accounted for to ensure robust estimates of total sap flux (Alvarado-Barrientos et al., 2013; Gebauer et al., 2008; Wullschleger and King, 2000). J_s at each measurement depth was used to calculate a weighted mean J_s according using radial fractions of the sapwood represented by each thermocouple and applying the assumed area in concentric circles bounded by the mid-point at each thermocouple extending toward the heartwood interface. Gap-filling of data was conducted on a sensor-by-sensor and tree-by-tree basis through generating simple linear regressions with the most parsimonious available data. Data gaps from a single depth within an individual were filled by creating a linear regression equation with an adjacent depth of the sample probe set. All gap-fill regression equations used no less than 2000 data points (equivalent to 20.8 days of point-measurements) and had an $R^2 > 0.9$.

We excluded the oaks from control plot C2 from the analysis of control vs treatment sap flux density, because even during the pre-treatment year it was apparent that they were poorly suited as control trees for the oaks being monitored in the other plots. This anomaly was seen in all three years of sapflow data collection, though different sensors were re-installed each year in freshly drilled holes at a slightly different position on each tree. A close examination of these trees led us to reject several hypotheses about what might cause these trees to have lower water usage – the plot is not drier than the other plots, does not have shallower soil and the oaks are all apparently healthy, have wide codominant crowns with no mid-day shading, and show similar radial growth rates to oaks in the other plots. More appropriate control trees were later selected, but not for the years of data presented in this manuscript.

S1c: Hydraulic Vulnerability Curves

Branch vulnerability curves were constructed for oaks and pines from the control plots in 2017. Distal pine branches of at least 40 cm length were collected using a shotgun, while similarly sized oak branches could only be collected by climbing to the lower canopy and using an extendable pole pruner. Branches were immediately put in water and at least three cuts were made under water to reduce any propagation of embolism. Branches were wrapped in damp paper towels, sealed in a plastic bag, and transported back to the lab. In the lab, branches were trimmed to 14 cm using multiple subsequent cuts on both ends underwater and the lateral branches trimmed (Torres-Ruiz et al., 2015). All branches were tested for open vessels by applying pressurized air to one end and placing the other end under water to determine whether air immediately passed through the segment (Ewers and Fisher, 1989). Only branch segments with no open vessels were used. Branch segments were vacuum infiltrated overnight by submerging them in filtered, degassed, distilled water at pH = 2 (to inhibit microbial growth) in a vacuum chamber.

Vulnerability curves were constructed using the centrifuge method (RC 5C Plus, Sorvall) with a modified rotor (Alder et al., 1997) to induce pressure. Foam pads were placed in the reservoirs to avoid sample dehydration while samples were in the rotor. Samples were spun for 3 min at rotor velocities corresponding to specific pressures (0 to -7 MPa) at the center of the segment. Before the first spin and following each subsequent spin, the hydraulic conductivity was measured using a hydrostatic pressure head to induce flow. Additional tubing was attached to the distal end of the segment and flow rate was measured using the SLI-Series Flow Meter (Sensirion, Staefa, Switzerland). Xylem area-specific hydraulic conductivity was calculated considering the volumetric flow rate, the hydrostatic pressure gradient, and the cross-sectional xylem area for each segment.

Supplemental measurements were made on separate branches using the bench dehydration method (Tyree et al., 1992). For bench dehydration tests, samples were harvested in the same manner, allowed to dehydrate on the benchtop for varying periods of time and then bagged and put in the dark for at least 3 h. Following this, water potential was quantified on three leaves from the sample and hydraulic conductivity measured using the hydrostatic pressure head. Samples were then flushed with positive pressure at 0.1 MPa for at least 30 min and then maximum conductivity measured on the same sample. The percentage loss in hydraulic conductivity was calculated from the maximum value for that sample as:

$$PLC = 100 \times (1 - (k_s/k_{smax}))$$

where PLC is the percent loss conductivity of the sample, k_s is the hydraulic conductivity of the sample and k_{smax} is the maximum measured conductivity of that sample.

Figure S1: Photos of the throughfall removal structures at Thompson Farm in Durham, NH.

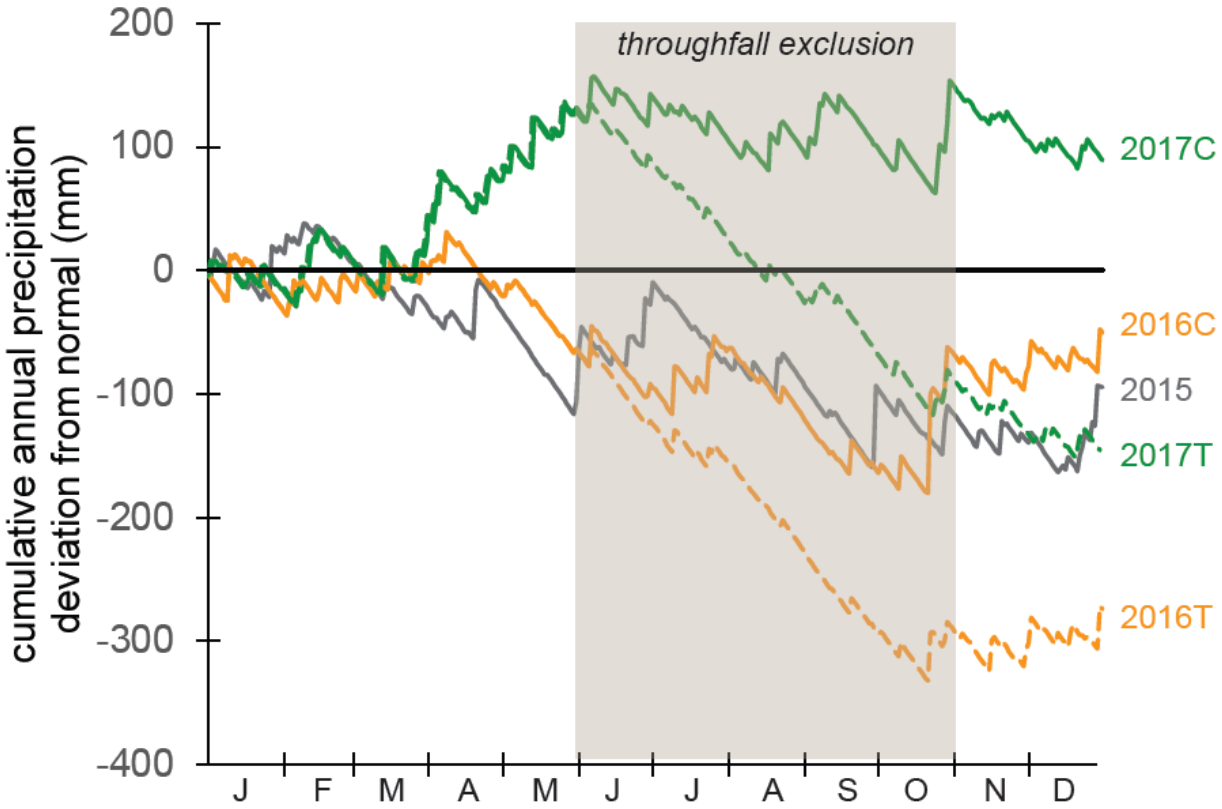

Figure S2. The deviation of each study year's cumulative precipitation from the 30-year normal period. Effective precipitation in the throughfall exclusion (T) plots (dashed lines) is estimated at 50% of ambient during the months throughfall exclusion is in effect. C indicates control plots.

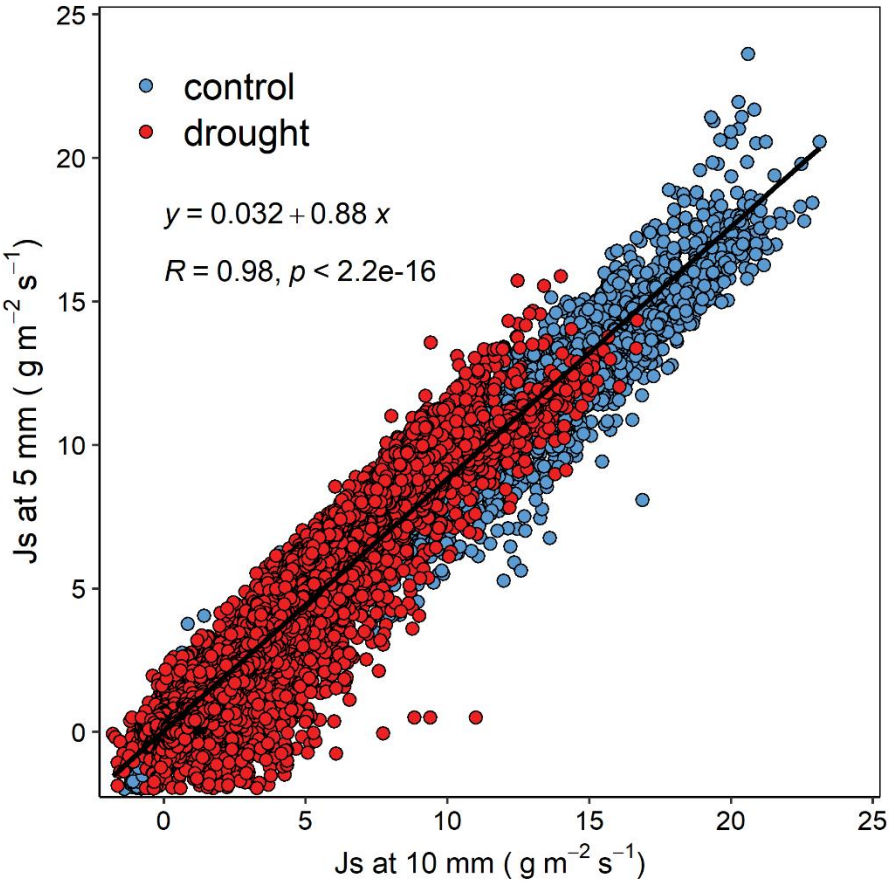

Figure S3: Linear regression for the sap flux density (Js) at the 5 mm depth (y-axis) as a function of Js at the 10 mm depth (x-axis) in *Quercus rubra* and *Q. velutina*. Data includes 9 trees on the 15-minute time step for a total n = 114,912 observations. This relationship was used to scale results from sensor probes with the outermost thermocouple at 10-mm depth to be directly comparable to those with the outermost thermocouple at 5-mm depth

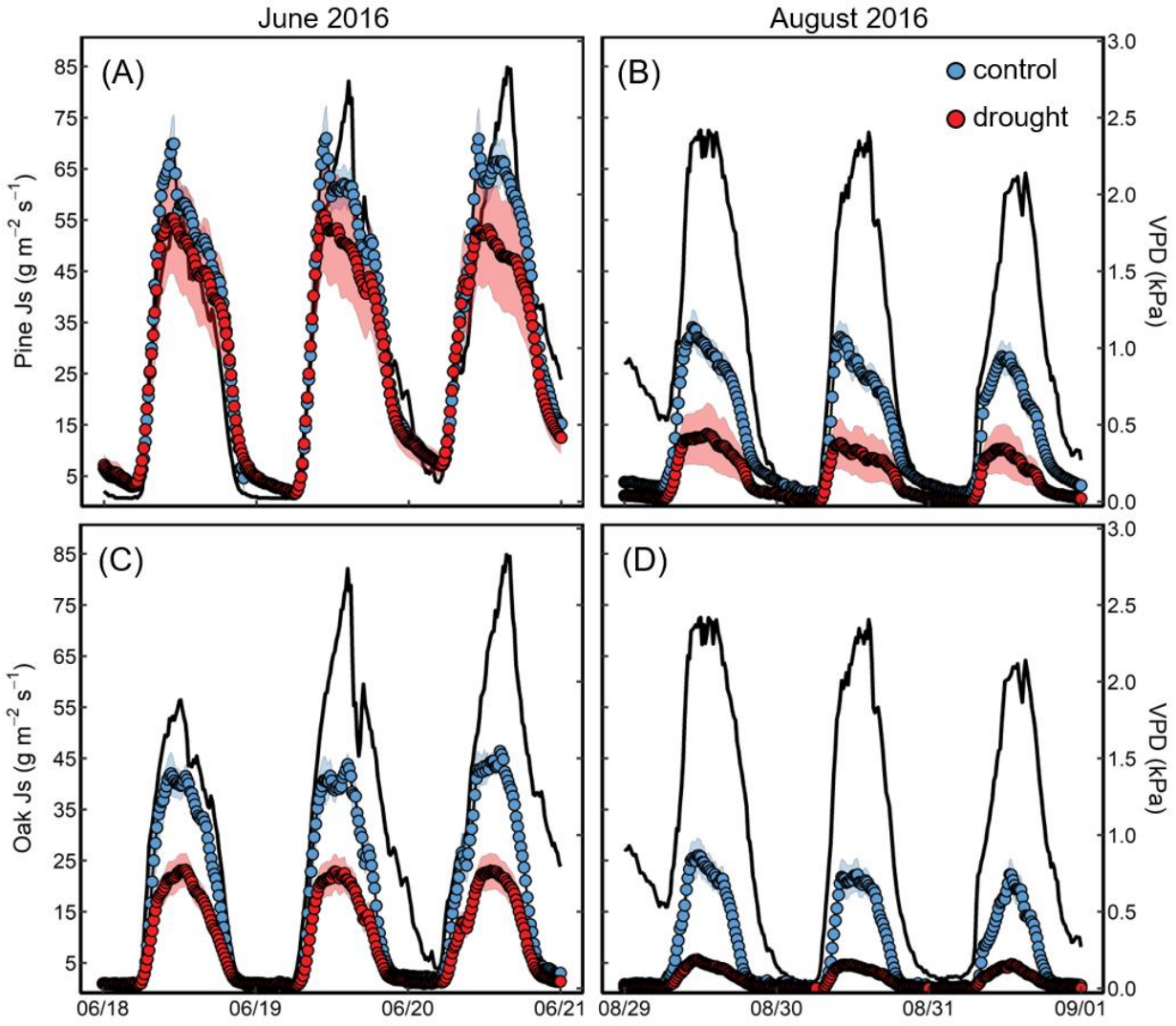

Figure S4. A high-temporal-resolution example of sapflux density (J_s) during the 2016 growing season, the first year of precipitation exclusion. Early and late season J_s shown for pine in panels (A) and (B) respectively; early and late season J_s for oak shown in panels (C) and (D) respectively. Trees within the control and drought treatment are indicated in blue and red circles respectively. Shaded area represents standard error for n=6 trees (n=3 in control oaks). The plain black line shows VPD over the course of each day.

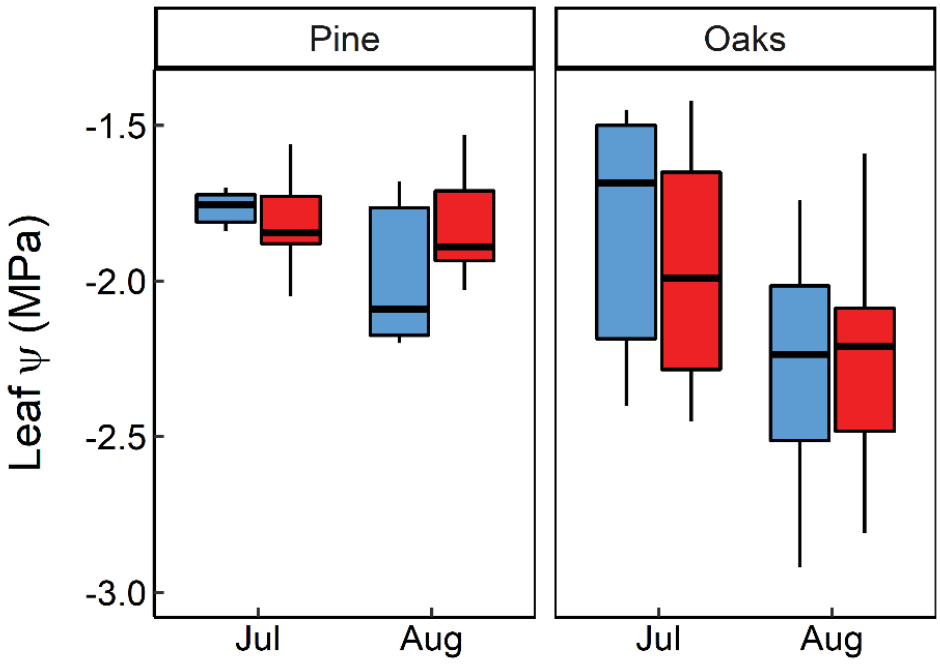

Figure S5. Leaf water potential in July and August 2016 comparing control (blue) and drought (red) treatments for pine and oak.

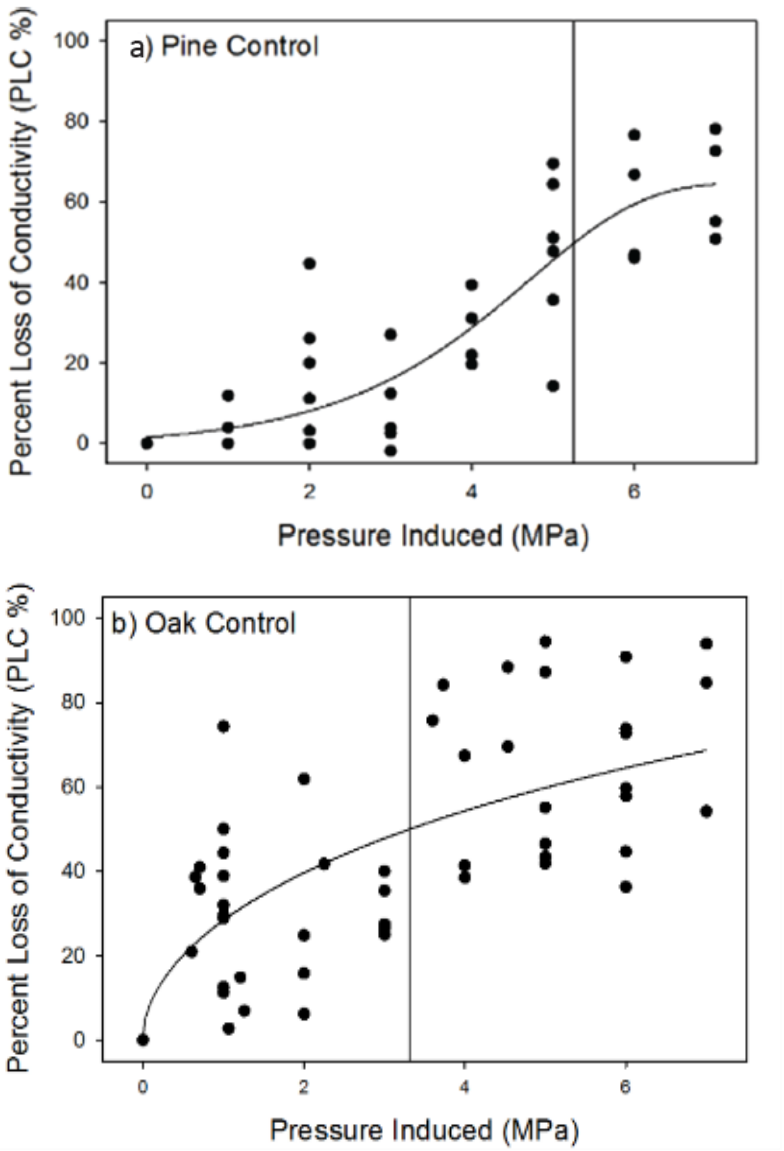

Figure S6. Hydraulic vulnerability curves for *P. strobus* (a) *Q. rubra* and *Q. velutina* (b) and branches collected from the control plots in 2017. Points represent individual measurements, and the best fit relationship is shown. The vertical line represents the pressure at which a 50% loss of conductivity occurred (P_{50}).

Table S1. Values for mean June sap flux density (J_s) by year, plot, and species. Oak data from plot C2 were not analyzed due to large pre-existing sap flux density differences relative to the other three plots, as explained in the main text of the document.

Year	Species	Treatment	Plot	June mean J_s	*n* days
2015	*Pinus strobus*	control	C1	37.30	20
			C2	39.90	20
		drought	T1	36.77	20
			T2	31.02	20
	Quercus spp.	control	C1	7.80	20
			C2	NA	NA
		drought	T1	7.41	20
			T2	3.93	12
2016	*Pinus strobus*	control	C1	27.31	24
			C2	31.90	24
		drought	T1	29.26	22
			T2	24.42	18
	Quercus spp.	control	C1	15.39	24
			C2	NA	NA
		drought	T1	10.21	24
			T2	8.13	25
2017	*Pinus strobus*	control	C1	26.60	10
			C2	37.44	16
		drought	T1	37.03	16
			T2	28.81	12
	Quercus spp.	control	C1	21.75	10
			C2	NA	NA
		drought	T1	16.01	17
			T2	14.17	12

Table S2. Summary statistics for mid-day water potential ANOVA testing for interaction effects for month (July, August), species (oak, pine), and treatment (control, drought) during the 2016 growing season. Differences between treatments for each species are considered significant at $p < 0.05$ (shown in bold).

source	df	sum of squares	*F* ratio	*p*
Month	1	0.7148	7.195	**0.01**
Spp	1	0.6985	7.031	**0.01**
Treatment	1	0.0009	0.009	0.93
Month x Spp	1	0.1876	1.889	0.18
Month x Treatment	1	0.1242	1.250	0.27
Sppx Treatment	1	0.0280	0.282	0.60
Month x Spp x Treatment	1	0.0005	0.005	0.94

Table S3. Summary statistics for gas exchange analyses of photosynthesis (A), stomatal conductance (g_s), and intrinsic water use efficiency (iWUE). A two-tailed *t*-test is used in the 2015 pre-treatment year, while one-tailed tests are reported for post-treatment years 2016 and 2017. Differences between treatments for each species are considered significant at $p < 0.05$ (shown in bold).

		A				**g_s**				**iWUE**			
		df	mean diff.	*t*	*p*	df	mean diff.	*t*	*p*	df	mean diff.	*t*	*p*
Pine	2015	8.3	-1.76	1.16	0.280	7.8	-0.03	1.55	0.161	9.2	14.68	-1.68	0.127
	2016	9.1	-1.9	1.85	**0.048**	7.8	-0.032	2.7	**0.014**	5.4	30.34	-2.53	**0.024**
	2017	6	-1.28	1.99	**0.047**	8	-0.016	2.09	**0.035**	10.0	-3.46	0.25	0.596
Oak	2015	7	3.05	-1.21	0.265	7	-0.010	-0.15	0.888	4.0	11.45	-0.88	0.427
	2016	4.9	-3.68	2.08	**0.046**	2.7	-0.048	1.7	0.099	2.4	16.05	-1.24	0.161
	2017	6.8	-1.63	-0.68	0.739	3.8	-0.058	-0.61	0.574	3.2	-5.33	0.36	0.628

References

Alder, N.N., Pockman, W.T., Sperry, J.S., Nuismer, S., 1997. Use of centrifugal force in the study of xylem cavitation. J. Exp. Bot. 48, 665–674. https://doi.org/10.1093/jxb/48.3.665

Alvarado-Barrientos, M.S., Hernández-Santana, V., Asbjornsen, H., 2013. Variability of the radial profile of sap velocity in *Pinus patula* from contrasting stands within the seasonal cloud forest zone of Veracruz, Mexico. Agric. For. Meteorol. 168, 108–119. https://doi.org/10.1016/j.agrformet.2012.08.004

Ambrose, A.R., Sillett, S.C., Koch, G.W., Van Pelt, R., Antoine, M.E., Dawson, T.E., 2010. Effects of height on treetop transpiration and stomatal conductance in coast redwood (*Sequoia sempervirens*). Tree Physiol. 30, 1260–1272. https://doi.org/10.1093/treephys/tpq064

Berdanier, A.B., Miniat, C.F., Clark, J.S., 2016. Predictive models for radial sap flux variation in coniferous, diffuse-porous and ring-porous temperate trees. Tree Physiol. 36, 932–941. https://doi.org/10.1093/treephys/tpw027

Burgess, S.S.O., Adams, M.A., Turner, N.C., Beverly, C.R., Ong, C.K., Khan, A.A., Bleby, T.M., 2001. An improved heat pulse method to measure low and reverse rates of sap flow in woody plants. Tree Physiol. 21, 589–598. https://doi.org/10.1093/treephys/21.9.589

Davis, T.W., Kuo, C.-M., Liang, X., Yu, P.-S., 2012. Sap flow sensors: Construction, quality control and comparison. Sensors 12, 954–971. https://doi.org/10.3390/s120100954

Durocher, M.G., 1990. Monitoring spatial variability of forest interception. Hydrol. Process. 4, 215–229. https://doi.org/10.1002/hyp.3360040303

Ewers, F.W., Fisher, J.B., 1989. Techniques for measuring vessel lengths and diameters in stems of woody plants. Am. J. Bot. 76, 645. https://doi.org/10.2307/2444412

Gebauer, T., Horna, V., Leuschner, C., 2008. Variability in radial sap flux density patterns and sapwood area among seven co-occurring temperate broad-leaved tree species. Tree Physiol. 28, 1821–1830. https://doi.org/10.1093/treephys/28.12.1821

Gotsch, S.G., Asbjornsen, H., Holwerda, F., Goldsmith, G.R., Weintraub, A.E., Dawson, T.E., 2014. Foggy days and dry nights determine crown-level water balance in a seasonal tropical montane cloud forest. Plant, Cell Environ. 37, 261–272. https://doi.org/10.1111/pce.12151

Helvey, J.D., 1967. Interception by eastern white pine. Water Resour. Res. 3, 723–729. https://doi.org/10.1029/WR003i003p00723

Knapp, A.K., Hoover, D.L., Wilcox, K.R., Avolio, M.L., Koerner, S.E., La Pierre, K.J., Loik, M.E., Luo, Y., Sala, O.E., Smith, M.D., 2015. Characterizing differences in precipitation regimes of extreme wet and dry years: Implications for climate change experiments. Glob. Chang. Biol. 21, 2624–2633. https://doi.org/10.1111/gcb.12888

Looker, N., Martin, J., Jencso, K., Hu, J., 2016. Contribution of sapwood traits to uncertainty in conifer sap flow as estimated with the heat-ratio method. Agric. For. Meteorol. 223, 60–71. https://doi.org/10.1016/j.agrformet.2016.03.014

Marshall, D.C., 1958. Measurement of sap flow in conifers by heat transport. Plant Physiol. 33, 385–396. https://doi.org/10.1104/pp.33.6.385

McIntire, C.D., Huggett, B.A., Dunn, E., Munck, I.A., Vadeboncoeur, M.A., Asbjornsen, H., 2020. Pathogen-induced defoliation impacts on transpiration, leaf gas exchange, and non-structural carbohydrate allocation in eastern white pine (*Pinus strobus*). Trees - Struct. Funct. in press. https://doi.org/10.1007/s00468-020-02037-z

Miller, D.R., Vavrina, C.A., Christensen, T.W., 1980. Measurement of sap flow and transpiration in ring-porous oaks using a heat pulse velocity technique. For. Sci. 26, 485–494. https://doi.org/10.1093/forestscience/26.3.485

Poyatos, R., Čermák, J., Llorens, P., 2007. Variation in the radial patterns of sap flux density in pubescent oak (*Quercus pubescens*) and its implications for tree and stand transpiration measurements. Tree Physiol. 27, 537–548. https://doi.org/10.1093/treephys/27.4.537

Renninger, H.J., Schäfer, K.V.R., 2012. Comparison of tissue heat balance- and thermal dissipation-derived sap flow measurements in ring-porous oaks and a pine. Front. Plant Sci. 3, 1–9. https://doi.org/10.3389/fpls.2012.00103

Steppe, K., De Pauw, D.J.W., Doody, T.M., Teskey, R.O., 2010. A comparison of sap flux density using thermal dissipation, heat pulse velocity and heat field deformation methods. Agric. For. Meteorol. 150, 1046–1056. https://doi.org/10.1016/j.agrformet.2010.04.004

Torres-Ruiz, J.M., Jansen, S., Choat, B., McElrone, A.J., Cochard, H., Brodribb, T.J., Badel, E., Burlett, R., Bouche, P.S., Brodersen, C.R., Li, S., Morris, H., Delzon, S., 2015. Direct x-ray microtomography observation confirms the induction of embolism upon xylem cutting under tension. Plant Physiol. 167, 40–43. https://doi.org/10.1104/pp.114.249706

Tyree, M.T., Alexander, J., Machado, J.-L., 1992. Loss of hydraulic conductivity due to water stress in intact juveniles of *Quercus rubra* and *Populus deltoides*. Tree Physiol. 10, 411–415. https://doi.org/10.1093/treephys/10.4.411

Vandegehuchte, M.W., Steppe, K., 2013. Sap-flux density measurement methods: working principles and applicability. Funct. Plant Biol. 40, 213–223. https://doi.org/http://dx.doi.org/10.1071/FP12233

Wullschleger, S.D., King, A.W., 2000. Radial variation in sap velocity as a function of stem diameter and sapwood thickness in yellow-poplar trees. Tree Physiol. 20, 511–518. https://doi.org/10.1093/treephys/20.8.511

Yi, K., Dragoni, D., Phillips, R.P., Roman, D.T., Novick, K.A., 2017. Dynamics of stem water uptake among isohydric and anisohydric species experiencing a severe drought. Tree Physiol. 37, 1379–1392. https://doi.org/10.1093/treephys/tpw126